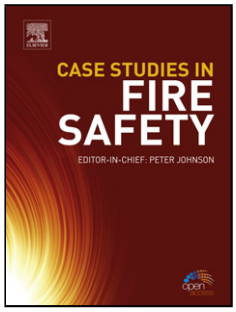

Title: Kinetic study and structural evolution of SON68 nuclear waste glass altered from 35 to 125null°C under unsaturated H_2O and D_2O^{18} vapour conditions

Authors: Rachid Bouakkaz, Abdesselam Abdelouas, Bernd Grambow

PII: S0010-938X(17)30525-5
DOI: https://doi.org/10.1016/j.corsci.2017.12.035
Reference: CS 7311

To appear in:

Received date: 27-3-2017
Revised date: 3-12-2017
Accepted date: 22-12-2017

Please cite this article as: Rachid Bouakkaz, Abdesselam Abdelouas, Bernd Grambow, Kinetic study and structural evolution of SON68 nuclear waste glass altered from 35 to 125x202f;deg;C under unsaturated H2O and D2O18 vapour conditions, Corrosion Science https://doi.org/10.1016/j.corsci.2017.12.035

Kinetic study and structural evolution of SON68 nuclear waste glass altered from 35 to 125 °C under unsaturated H_2O and D_2O^{18} vapour conditions

Rachid Bouakkaz*, Abdesselam Abdelouas, Bernd Grambow

SUBATECH – Ecole des Mines de Nantes-CNRS/IN2P3-Université de Nantes, 4, rue Alfred Kastler, B.P. 20722, 44307 Nantes, France
*corresponding author: Rachid.Bouakkaz@subatech.in2p3.fr
rachidbouakkaz@yahoo.fr

Graphical abstract

R. Bouakkaz,* A. Abdelouas, B. Grambow,

PCCP. 2017, **XX**, YY

The SON68 glass was vapor hydrated under H_2O and D_2O^{18} at (35–125 °C) and (92–99.9%) relative humidity, and then leached in COx water. The hydration activation energy value is between 34 and 68 kJ mol^{-1}. D_2O^{18} diffusion coefficient is 2.3×10^{-19} m^2 s^{-1}.

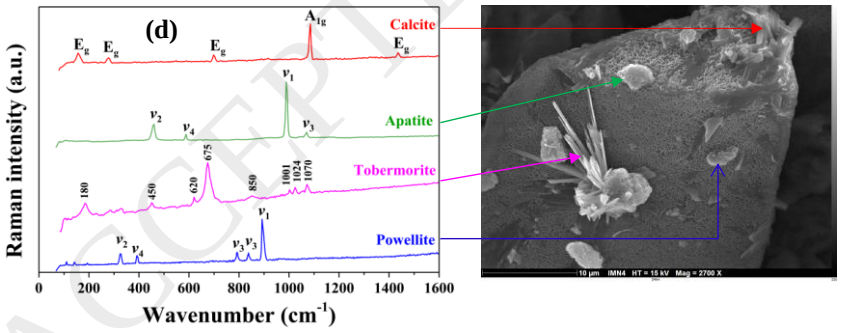

Abstract

The French reference SON68 nuclear waste glass corrosion under H_2O and D_2O^{18} atmosphere was investigated at 35−125 °C and different relative humidities (92 - 99.9%). The hydration kinetic was followed by FTIR and solid characterization was achieved using SEM/EDX, Raman and TOF-SIMS. The water diffusion coefficients in the glass ranged from 8.7×10^{-22} to 5.3×10^{-19} m^2 s^{-1}. The alteration products were calcite, apatite, powellite and tobermorite. Pre-hydrated glass alteration in synthetic groundwater at 50 °C showed an instantaneous release of elements from the surface, making it important to evaluate well the vapour hydration period of the glass.

Keywords: SON68 glass, vapour hydration, nuclear waste disposal, deuterium, Raman, SIMS

1. Introduction

In many countries using nuclear energy high-level wastes resulting from the reprocessing of nuclear spent fuel is being confined in a highly-resistant glass matrix. In France, the resulting highly radioactive glass, named R7T7, is cooled in stainless steel canisters and stored on-site waiting for final geological disposal. For geological disposal the waste package will be encapsulated in carbon steel container and then sent to a multi-barrier underground disposal facility located in an argillaceous Callovo-Oxfordian (COx) layer. This confinement system should limit both the glass alteration by surrounding ground waters and the release of the radioactive elements from the glass matrix, although the alteration of the glass by surrounding ground waters cannot be excluded for long-term. It is expected after closure of the disposal facility that the glass will be firstly in contact with water vapour before complete saturation of the void spaces. In fact, the anoxic corrosion of metallic components will lead to a massive production of hydrogen that will probably prevent a fast saturation of the glass container with the surrounding ground waters. Consequently, a phenomenon of glass vapour hydration may occur for several thousands of years before the glass becomes completely submerged by groundwater.

Various studies have been conducted to better understand the hydration of nuclear glasses [1−5] and their natural analogues such as obsidian [6−11]. During the hydration process, a thin film of water is firstly sorbed or condensed on the surface of the glass [12]. The thickness of the sorbed film of water mainly depends on the temperature and relative humidity (RH), the latter was controlled by varying the concentration of NaCl in the solution [13]. The condensed water diffuses and reacts via a hydrolysis and ion exchange mechanism. This leads to the transfer of glass components to the glass surface. The glass surface-area-to-liquid volume (*S/V*) ratio is estimated to be high under water vapour hydration (in the order of 10^8 m^{-1}) [12]. This estimation is based on the sorption curve of water on the SRL glass as a function of the relative humidity. The thin film of water became rapidly saturated with dissolved glass constituents leading for certain glass compositions to higher local pH values and then the increase of solubility of the silicate glasses network. An alteration layer grows on the corroded glass surface; it is mainly composed of hydration gel, pore water and crystalline alteration products. The thickness of the alteration layer and the nature of secondary phases precipitated on the external surface depend on experimental conditions (time, temperature, RH, pH) and glass composition.

In the hydration experiments conducted at 200 °C by Gong et al. [14] with the inactive simulated French nuclear waste glass SON68, the authors investigated the hydration layer structure and the formation of secondary phases. The main secondary phases identified using cross-section (AEM/SEM/HRTEM) analyses were analcime, tobermorite, apatite, weeksite and other Ca-Si phases such as gyrolite, afwillite and nekoite. The precipitation of Si-rich phases can largely enhance the rate of glass alteration via consumption of Si from the small water film on the glass surface, which push the system into unsaturated conditions with respect to dissolved silica [15,16]. Numerous crystalline phases such as calcite, powelite, analcime and tobermorite were also identified by Neeway et al. [4] on the surface of SON68 glass hydrated at 175 °C and 92% RH. For the hydrated sample at 90 °C and 92% RH for 512 days, the authors measured by TOF-SIMS technique an alteration depth of 600 nm which represents an alteration rate of 3×10^{-3} g m^{-2} d^{-1} if one assumes that the rate is constant with time. This value is ten times higher than that obtained for glass leaching experiments in pure water at the same temperature [17]. The effect of pH on the hydration of SON68 glass was studied by Aït Chaou et al. [18]. Experiments were carried out at 175 °C under different atmospheres (NH_3 and H_2S) and compared with those obtained under air. It has been shown that the glass hydration is ten times higher at high pH conditions obtained under ammonia atmosphere than under hydrogen sulphide leading to acidic conditions. The increase in glass hydration rate under NH_3 is due to the high solubility of silica associated with the precipitation of Si-consuming secondary phases such as analcime, smectite and tobermorite. In contrast, under H_2S atmosphere only a gel-like phase was identified leading to a lower hydration rate even though under air.

The present work aims to study the behaviour of SON68 glass under unsaturated environment and at temperatures ranging from 35 to 125 °C, which includes the range of temperature foreseen in the French concept of HLW deep geological disposal. The glass composition is given in **Table 1**. In a previous work by Bouakkaz et al. [19] we studied the leaching of SON68 glass in silica-rich synthetic COx water at 35, 50 and 90 °C. We determined the rates of glass corrosion for each temperature, the mechanisms responsible for glass corrosion and the different secondary phases formed. We have judiciously chosen these temperature values because they represent: the expected temperature shortly after the closing of the disposal galleries (90 °C) ; the expected temperature after the breach of the overpack containers (50 °C) and the temperature close to Callovo-Oxfordian formation at 500 m deep (35 °C) [20]. RH values range between 92 and 99.9% all situations. Additional hydration experiments were

then carried out at 90 and 125 °C for 95% RH in the presence of deuterated water in order to study, using TOF-SIMS analysis, the penetration of water vapour in the glass and the mechanisms responsible for the glass alteration. Finally, to simulate the expected storage conditions, all hydrated monoliths were altered in COx water at 50 °C. Analyses of the alteration solution by ICP-MS allow evaluating the release of elements present in the alteration layers.

2. Experimental

2.1. Materials and procedure

The French inactive SON68 glass was provided by the French Atomic Commission (CEA) (**Table 1**). Thin glass monoliths with dimensions of (1 × 1 × 0.1 cm) were cut from a glass block and polished to 1 µm until becoming transparent to light. The glass scraps were crushed and fractioned by sieving. The resulting glass powder (ϕ<32 µm) and monoliths were carefully washed with ethanol during 1h using the ultrasonic cleaner to remove fines.

Glass hydration experiments were carried out in a stainless steel autoclave with a Teflon liner (40ml) [4,5]. The glass monoliths and powder were placed separately on a Teflon holder. In order to prevent temperature gradients that may cause vapour condensation on the surface of glass samples during heating and cooling processes, the autoclave was placed in an aluminium container (2 cm thick) which serves to homogenize the temperature inside the autoclave.

Tests were performed at temperatures ranging from 35 to 125 °C and relative humidities values ranging from 92 to 99.9%. The relative humidity was controlled by varying the concentration of NaCl in the solution (8 mL) placed underneath the glass holder. Thereby, saline solutions of 2.23; 1.03; 0.6 and 0.04 mol_{NaCl}/kg_{H2O} were used to obtain 92; 95; 98 and 99.9 % of RH, respectively, considering that for the used salinities the RH depends only little on temperature. The flowchart in **Fig. 1** gives a summary of each experiment with the operational conditions. The glass monoliths in the experiments 10 and 11 are hydrated in the presence of water containing 20 wt% D_2O^{18}. In experiments 16 and 17, the glass powder was not added in order to compare with hydration experiments in the presence of D_2O^{18}.

Samplings were performed at time intervals between 7 and 30 days. To do this the autoclaves were taken out of the oven and left to cool for 6 hours at room temperature to minimize

possible vapour condensation on the surface of glass samples. Glass monoliths were removed from the autoclaves, weighted and then analysed using Fourier Transform-Infrared (FTIR) spectroscopy between 4000 and 2500 cm^{-1}. The saline solution was weighted and changed after pH measurements. The volume of the saline solution was controlled for each sampling and the loss was estimated to be less than 1 wt%.

In order to simulate the expected storage conditions, hydrated glass monoliths (1 cm × 1 cm × 0.1 cm) were altered at 50 °C in synthetic Callovo-Oxfordian (COx) water (**Table 2**). The leaching experiments were carried out in static mode in Teflon vials containing 10 mL of solution giving a ratio of glass surface to solution volume (*S/V*) ratio near 22 m^{-1}. A volume of 0.5 mL of the solution was removed from each vial after 1, 4, 11, 29 and 78 days of alteration. After pH measurements at 25 °C, the solutions were acidified with 0.2% HNO_3 and then stored at 4 °C before analysing by ICP-MS. A non-hydrated glass monolith (Blank) was also altered for comparison with the hydrated glass. The normalized mass loss NL (gm^{-2}) was calculated from the release of B, Li, Cs and Mo according to the following relation:

$$NL_i = \frac{C_i}{X_i \times (S/V)} \qquad (1)$$

With C_i the concentration of the component *i* in the solution in g m^{-3}, X_i the mass fraction of component *i* in the pristine glass and (*S/V*) is the glass surface area to solution volume ratio in m^{-1}.

2.2. Analytical methods

The evolution of glass hydration over time was monitored using FTIR spectroscopy, according to protocols developed in [4,5,18,22]. Transparent glass monoliths were analysed using 8400 Shimadzu between 4000 and 2500 cm^{-1}. The obtained spectra were deconvoluted with five Gaussian using Origin 8.0 software (OriginLab).

The morphological and chemical analyses of hydrated glass powder and monoliths were performed using (JSM 5800 LV, 15 kV) scanning electron microscope (SEM) coupled with energy-dispersive X-ray spectroscopy (EDX). In order to obtain a better resolution of the K-lines for lighter glass components (Si, Al and Ca), the glass was coated with a thin layer of

carbon for surface imagining. The final compositions were calculated assuming the stoichiometry of the oxides and normalization to 100%.

Hydrated glass powder and monoliths were also analysed by micro-Raman spectroscopy to identify glass corrosion products. A high resolution T64000 Tobin-Yvon/LABRAM spectrometer equipped with a 600 lines/mm diffraction grating was used. The spectrometer is equipped with an Olympus microscope (× 100 objectives) and Ar^+–Kr^+ laser (514 nm exciting line). Single spectra were obtained in the wavenumber 100–2200 cm^{-1} region with an integration time of 600 s. Measurements were carried out at very low laser power (5 mW) to avoid any deterioration of the sample.

The time-of-flight secondary ion mass spectroscopy (TOF-SIMS) technique was also used to obtain elemental profiling and corrosion layer thickness. Profiles were obtained using an IONTOF GmbH TOF SIMS instrument by alternating abrasions and analyses. Abrasions were run with a 2 keV primary O_2^+ ion beam on an area measuring 300 × 300 μm^2. Analyses were carried out using a focused Bi^+ primary beam at 25 KeV on an area measuring 100 × 100 μm^2.

At the end of experiments, hydrated glass monoliths were leached in synthetic Callovo-Oxfordian (COx) water at 50 °C. Leaching solutions were analysed at SUBATECH laboratory using a PQ-Excel VG-Elemental Inductively-Coupled Plasma-Mass Spectroscopy (ICP-MS) to monitor the evolution of B, Li, Cs and Mo concentrations over time. The analytical uncertainty was between 4 and 9%.

3. Results

3.1. Glass hydration kinetics

An example of the evolution with time of a typical FTIR spectrum for a sample hydrated at 90 °C and 99.9 RH for 653 days may be seen in **Fig. 2**. Other experiments show a similar spectral evolution. All spectra have been normalized to their maximum (Imax) and minimum (Imin) intensity. To determine the kinetics of SON68 glass hydration, we have chosen to follow the evolution of the band at 3595 cm^{-1}, which corresponds to the vibration of silanol group (SiOH) [23]. In order to distinguish the silanol group from the molecular water, we performed for each spectrum a deconvolution with five Gaussian using the Origin 8.0

software (OriginLab). The different bands and their contributions are detailed in Aït Chaou et al. [6,18].

3.1.1. Effect of temperature on the glass hydration

Fig. 3.a–c shows the growth of the absorbance of the SiOH peak at 3595 cm^{-1} as a function of time at different temperatures for SON68 glass hydrated under relative humidities of 92, 95, and 98%. The absorbance values were normalized using the SiOH absorbance of the pristine glass (at time zero). Higher temperatures should increase the surface reactivity and the diffusion of water into the glass network or ion exchange and then the hydration rate [5]. The temperature should also favour the hydrolysis of the glass network bonds by molecular water which leads to the dissolution of silica and the formation of silanol groups. In **Fig. 3.**, the evolution of the absorbance increases linearly with time until a slowdown in the glass hydration with the appearance of a plateau after 593 and 652 days for the hydrated samples at 125 °C and 90 °C, respectively.

It is possible to calculate the activation energy of SON68 glass hydration process. To do this, the glass hydration rate *HR* (g m^{-2} d^{-1}) can be calculated from the hydration layer thickness. Calculations of the alteration layers thicknesses (*Alt*) can be based on a correspondence between the FTIR measurements and SEM observations from a hydrated sample. A conversion factor of 0.09 units of absorbance was obtained for 1µm of alteration thickness. This factor was also obtained for other types of borosilicate glass: intermediate-level CSD-B nuclear glass [6] and a borosilicate glass [4,5]. This result has therefore allowed us to estimate the thickness of the alteration layer directly from FTIR measurements that give the absorbance of the SiOH peak at 3595 cm^{-1}. The alteration layer thickness could not be measured by TEM in this work. However, SEM and SIMS analysis of the sample #11 hydrated for 593 days at 125 °C and 95% RH in the presence of D_2O^{18} (20%); and of the sample #17 hydrated for 322 days at 125 °C and 95% RH (without glass powder) consolidate this approach of equivalence hydration layer thickness and degree of absorbance (see section 3.3.1.2).

The evolution of the alteration layers thicknesses obtained from FTIR analysis for each SON68 glass samples over time is shown in **Fig. 4**a. A summary of layers thicknesses obtained by FTIR, SEM and SIMS is given in **Table 3**, which shows the complementarity

between these three techniques at different experimental conditions. The alteration layers thicknesses increase steadily before stabilizing from 593 days for samples hydrated at 125 °C, and from 652 days for samples hydrated at 90 °C. For samples hydrated at 35 and 50 °C, the plateau is not yet reached. The alteration layer thickness of the sample #13 hydrated for 482 days at 90 °C and 99.9% RH is about 2.3 µm. This value is higher than that obtained in leaching experiments in batch reactor under silica saturation conditions [19]. After 485 days leaching at 90 °C, the corrosion layer thickness is about 1 µm. This difference can be explained by both the saturation of solution in silica for leaching experiments, and by the local pH in contact with the glass, which is expected to be higher in hydration experiments. The second hypothesis is further supported by the work of Aït Chaou et al. [18]. The authors studied the hydration of SON68 glass at 175 °C under different atmospheres to determine the effect of pH on the glass hydration. The results showed that hydration of the glass under a highly alkaline atmosphere (NH_3 atmosphere) is two times higher than that obtained by Neeway et al. [4] under air, and ten times higher than that obtained in a more acidic atmosphere (H_2S atmosphere). Abrajano et al. [2] showed that the alteration of natural and nuclear glasses in vapour conditions leads to a rapid precipitation of secondary phases. Thus, alteration layers developed under the same temperature are less thick when the glasses are altered in pure water.

The rate of glass hydration *HR* (g m^{-2} d^{-1}) can be calculated for several hydration times from the hydration layers thickness determined previously by FTIR technique (in µm d^{-1}) then by multiplying this value by the SON68 glass density (2.63 g cm^{-3}). The evolution of *HR* (g m^{-2} d^{-1}) as a function of time for different temperatures and relative humidity values is illustrated in **Fig. 4**b. The average initial rates of glass hydration HR_0 values obtained from the linear part of each curve (before the appearance of the plateau) are given in **Table 4**. For samples #09 and #14 hydrated at 35 and 50 °C respectively, the plateau is not yet reached. The initial hydration rates are 1.1 (±0.1) × 10^{-3}, 2.2 (±0.2) × 10^{-3}, 8.2 (±0.8) × 10^{-3} and 1.1 (±0.1) × 10^{-2} g m^{-2} d^{-1} for 35, 50, 90 and 125 °C, respectively. The hydration rates decrease then with time for samples hydrated up to 90 °C. The average hydration rates $HR_{L\text{-}T}$ obtained from the appearance of a plateau and the end of the experiments were: 1.4 (±0.1) × 10^{-3} and 1 (±0.1) × 10^{-3} g m^{-2} d^{-1} for 90 and 125 °C, respectively. The slowdown of the glass hydration rate remains for the moment without explanation but the hydration rate may be explained by slowing of water diffusion with increasing layer thickness. At the end of experiments, the rate of glass hydration at 90 °C is around one order of magnitude higher than that obtained at 35

°C. The hydration rate obtained at 90 °C is consistent with that obtained by Neeway et al. [4] at the same temperature and 92% RH after 512 days, which is on the order of 3×10^{-3} g m^{-2} d^{-1}.

The dependence of the linear hydration rate, calculated from FTIR, SEM and SIMS data, on the temperature follows an Arrhenius law. The logarithm of the glass hydration rate *Ln HR* (g m^{-2} d^{-1}) versus the inverse of the absolute temperature is plotted in **Fig. 5**a. The apparent activation energy (*Ea*, J mol^{-1}) can be obtained from these plots using the Arrhenius equation:

$$k = A \times exp\left(\frac{-Ea}{RT}\right) \quad (2)$$

Where *k* is the rate constant (in this case the rate of glass hydration *HR* g m^{-2} d^{-1}), *A* is the Arrhenius parameter (g m^{-2} d^{-1}), *R* is the gas constant (8.314 J K^{-1} mol^{-1}) and *T* is the temperature in Kelvin (*K*). Applying the integrated form of equation (2) the slope of these plots has the value (–*Ea*/*R*).

The activation energy value is about 34 (±4) kJ mol^{-1}. This value is close to that obtained by Neeway [24] who studied the SON68 glass hydration at temperatures between 125 and 200 °C for 92% RH. Author calculated an activation energy of 43 kJ mol^{-1} (from FTIR) and 47 kJ mol^{-1} (from TEM). On the other hand, the samples #07 and #14 hydrated at 90 and 50 °C for 92% RH, respectively, show good agreement with the results of Neeway et al. [4] (**Fig. 5**b).

The water diffusion through the glass follows also an Arrhenius law. The diffusion coefficient of water (D_{H2O}) is obtained from the evolution of the alteration layer thickness (Alt_i) of sample (*i*) as a function of the time square root, for the period before the appearance of a plateau (**Fig. 6**a). The evolution of the layer thickness with the square root of time is almost linear for all samples, which indicates that the glass hydration is controlled by a diffusion process.

The diffusion coefficient of water in the glass (D_{H2O}) is calculated from the equation based on the first Fick law by assuming that the diffusion is the limited reaction [25]:

$$Alt_i = 2\sqrt{\frac{D_{H2O} \times t}{\pi}} \quad (3)$$

Where *t* is the time required to form the alteration layer thickness (Alt_i).

The apparent diffusion coefficient of water for sample #11 hydrated to 593 days at 125 °C and 95% RH in the presence of D_2O^{18} (20%) is about 5×10^{-19} m^2 s^{-1}, this value is close to that obtained from TOF-SIMS profile (see section 3.3.1.2). The values of D_{H2O} for the different samples are listed in **Table 5**. The diffusion coefficient at 35 °C of 8.7×10^{-22} m^2 s^{-1} is two orders of magnitude lower than that obtained at 90 °C (7.5×10^{-20} m^2 s^{-1}). Such a difference of two orders of magnitude is also noticed by Chave et al. [26] for the aqueous alteration of SON68 glass between 30 and 90 °C and by Rébiscoul et al. [27] for the alteration of soda-lime borosilicate glass between 12 and 60 °C.

The values of D_{H2O} obtained at 90 °C in this work are relatively high compared to those obtained for SON68 dissolution in silica rich solutions. Ferrand et al. [22] reported diffusion coefficient of 2×10^{-22} m^2 s^{-1} for the SON68 glass altered at 90 °C in a Si-saturated (240 ppm) synthetic solution. Likewise Chave et al. [26] obtained similar results for SON68 glass at pH 9 and 150 ppm Si (1.6×10^{-22} m^2 s^{-1}). The expected high pH of the condensed water film formed on the glass surface may have induced the formation of a porous and less compact gel layer in comparison to those formed in batch experiments.

The activation energy of water diffusion is obtained by plotting Ln (D_{H2O}) (m^2 s^{-1}) versus the inverse of temperature. At 50 °C, D_{H2O} value has been estimated at 95% RH as the average of that obtained at 92% RH (sample #14) and 98% RH (sample #15). This estimation is based on the evolution of the mass of water retained on the glass as a function of relative humidity, which increases in linear manner between 92 and 98% RH (see next section). The activation energy is equal to 68 kJ mol^{-1}, it is two times higher than that obtained from the hydration rate values (**Fig. 5**a). The same was observed by Chave et al. [26]. The authors obtained activation energies of 36.7 kJ mol^{-1} from the glass kinetic rates calculated from the elemental release and 86.3 kJ mol^{-1} from the water diffusion coefficients. It is important to notice that the diffusion coefficients are apparent because the water diffusion is associated with surface reaction including hydrolysis, condensation and phase precipitation. We may then suggest that glass vapour hydration is a resultant of water diffusion and surface reaction such as it was demonstrated by Bouakkaz et al. [19] for SON68 glass altered in Si-enriched clay water.

3.1.2. Effect of relative humidity on the glass hydration

Fig. 7a shows the growth of the absorbance of the SiOH peak at 3595 cm^{-1} as a function of time and relative humidity for SON68 glass hydrated at 90 °C. The glass hydration increases with relative humidity and also with time. This increase is due to the increase of water monolayers number which enhances the adsorption of water on the glass surface. Neeway et al. [4] showed that the glass hydration becomes more important for relative humidity values above 85%. The diffusion coefficient of water D_{H2O} through the glass is plotted in **Fig. 7**b versus RH for samples hydrated at 90 °C for 445 days. The calculated values of D_{H2O} are: 4.9 (±0.4) × 10^{-20} , 7.5 (±0.6) × 10^{-20} , 1.2 (±0.1) × 10^{-19} and 1.6 (±0.1) × 10^{-20} m^2 s^{-1} for samples hydrated under 92, 95, 98 and 99.9 % RH. The diffusion of water in the glass increases with RH in particular starting from 95% RH value.

The evolution of the mass of water retained on the glass monoliths surface as a function of the relative humidity is plotted for different time intervals in **Fig. 7**c. All glass monoliths have been weighed before hydration and after each sampling using a precision balance with an accuracy of 10^{-5} g. The difference in mass is considered to be the amount of water retained. It is found that the amount of water retained on the glass surface increases linearly between 92 and 98% RH for each sampling. This increase becomes remarkable above RH values of 98%. It is particularly more significant when the hydration time increases. In fact, for the first sampling (7 days) the deviation of the curve at 98% RH is less important. The increase is however almost exponential for 445 days. Thus this phenomenon can be attributed to the absorption of water in the alteration layer which develops during hydration, but also to the water condensation in the gel porosity for supersaturation values in relative humidity (Above 98% RH). In fact, the number of water monolayers absorbed on the glass increases exponentially when the relative humidity exceeds 98%. This phenomenon has been further demonstrated by Ebert et al. [12], who observed (for high values of relative humidity (>90%)) an inflection point in a graph of the number of water monolayers as a function relative humidity calculated for the SRL 165 nuclear borosilicate waste glass.

3.2. Analysis of hydrated glass by SEM/EDX and Raman spectroscopy

We chose to analyse samples while the experiments continue to run. To do this, the half of each sample is removed from the autoclave, the quarter is destined for analysis and the other quarter to alteration in solution. SEM micrographs of hydrated samples are shown in **Fig. 8**a–c, which illustrates glass monoliths hydrated at different conditions: (a) 35 °C and 95 %

RH to 654 days; (b) 50 °C and 98 % RH to 490 days; (c) 90 °C and 95% RH to 652 days. Different precipitates which abundance and chemical composition vary depending on the temperature are formed on the surface. The corresponding EDX spectra show an enrichment of the surface in Ca at all temperatures. In addition, P and Mo are identified at 90 °C (**Fig. 8**c), suggesting the presence of molybdate and phosphate [19].

Analyses by Raman spectroscopy revealed the presence of calcite on the glass surface hydrated at 35 and 50 °C. Calcite, apatite and powellite minerals are identified at 90 °C. These minerals were previously observed for the hydration of SON68 glass [4,14] and for the leaching of SON68 glass in silica-rich conditions for the same temperature range [19].

Glass powders and monoliths hydrated together in the autoclave showed the formation of the same precipitates on their surface. A SEM micrograph of glass powder hydrated after 593 days at 125 °C and 95% RH can be seen in **Fig. 8**d. The corresponding Raman spectra confirm the presence of calcite, powellite, apatite and tobermorite.

Calcite ($CaCO_3$) and powellite ($CaMoO_4$) minerals can incorporate trivalent actinides (Am, Cm) and lanthanides (La, Nd) [28,29]. Apatite is a calcium phosphate compound with a chemical formula of $Ca_5(PO_4)_3X$, where X can be a F^- (fluorapatite), Cl^- (chlorapatite) or an OH^- ion (hydroxyapatite). The orthophosphates ions can be able to form aqueous complexes with most the rare earth elements (REE) and the transition metals [30]. Tobermorite is a calcium silicate hydrate (C–S–H) with the chemical formula ($Ca_5Si_6O_{16}(OH)_2.nH_2O$). It was also identified during SON68 glass hydration at high temperatures [4,14]. Tobermorite has reputation to be a good adsorbent of alkali and alkaline earth elements via ion-exchange [14]. It also has a capacity to incorporate Eu(III) which is considered to be analogue for trivalent actinides [31].

3.3. Isotopic tracing by D_2O^{18} of SON68 glass hydration

As mentioned previously, two hydration experiments of SON68 glass using D_2O^{18} as an isotopic tracer were conducted to study, using TOF-SIMS analysis, the penetration of water into the glass. A solution spiked with D_2O^{18} (D_2 = 98% and ^{18}O = 97%) at 20 wt%, provided by (Cambridge Isotope Laboratories, INC), was used. Experiments were conducted at 90 °C and 125 °C under 95% RH. To control the RH, the activities of pure water and the mixture of

H_2O and D_2O^{18} in NaCl are considered to be the same. This assumption is supported by the work of Jakli [32], who studied the effect of H_2O–D_2O mixture on the molar volume of the aqueous solutions of LiCl, NaCl, KCl and CsCl at different temperatures. The author showed that this effect becomes almost negligible from 35 °C for a mass concentration of NaCl between 0.55 and 27.5% regardless of the H_2O–D_2O mixture. Thus, saline solution of 1.03 $mol_{NaCl}/kg_{(H2O\text{-}D2O)}$ is used to ensure a value of 95% RH. Experiments were run for 766 days; they correspond to experiments 10 and 11, respectively (see **Fig. 1**).

3.3.1. Results

When H_2O and D_2O^{18} are mixed, HDO^{16} and HDO^{18} species are formed:

$$H_2O + D_2O^{18} \longrightarrow HDO^{16} + HDO^{18}$$

The equilibrium constant of this reaction in aqueous NaCl solution and/or H_2O changes very slightly relative to that in vapour phase [33]. The author studied the distribution of H_2O, HDO and D_2O in vapour and liquid phases in pure water and aqueous solution systems between 0 and 100 °C and showed that the vapour pressure of HDO is slightly less than that of H_2O and D_2O. Gupta et al. [34] used the FTIR technique to study the species formed on the porous silica surface after exposure to saturated H_2O and D_2O at different temperatures. FTIR spectra showed that these two molecules are dissociated during their adsorption at 27 °C to form SiOH and SiOD, respectively (hydrolysis). The symmetric stretching ν_1 mode of SiO−H appears at 3680 cm^{-1} while that of SiO−D is observed at 2707 cm^{-1}. The authors also observed, from 127 °C, the formation of Si−O−Si species whose vibration mode is located between 900 and 1100 cm^{-1} (condensation). The overlap of the peak corresponding to the SON68 glass matrix and that of SiOD does not allow to follow the absorbance evolution of the SiOD peak over time. The glass hydration kinetic in the presence of D_2O^{18} (20%) is therefore ensured by monitoring the evolution of the peak at 3595 cm^{-1} which attributed to the vibration of SiOH group (e.g. Aït Chaou et al. [6]).

3.3.1.1. Effect of temperature and comparison between experiments in the presence of pure H_2O and mixture H_2O and D_2O^{18} (20%)

Fig. 9a shows the growth of the absorbance of the peak at 3595 cm^{-1} as a function of time for SON68 glass hydrated at 90 and 125 °C under 95% RH and in the presence of a saline solution containing D_2O^{18} (20%). The glass hydration seems to follow a square-root time-

dependent rate law (**Fig. 6**a). As it has been observed previously, the glass hydration is significantly higher at 125 °C than at 90 °C.

Fig. 9b and c show the growth of the absorbance of the peak at 3595 cm^{-1} as a function of time for SON68 glass hydrated at 90 and 125 °C, respectively, for a relative humidity of 95% in vapour phase of pure water and in the presence of D_2O^{18} (20%). It is noted that the glass hydration at 90 °C is almost the same in both environments whereas at 125 °C, in the presence of D_2O^{18} (20%), the glass hydration is slightly higher than that obtained in vapour phase not enriched in deuterium. This change may just be related to FTIR measurements error (around 10%).

This result suggests that the alteration thicknesses developed under different environments are slightly different and that the presence of D_2O^{18} does not seem to affect the glass hydration. This is in agreement with results obtained by Anovitz et al. [35] on the hydration of obsidian glass at 150 °C and 100% RH under H_2O, H_2O^{18} and D_2O. The alteration thicknesses measured by SIMS technique for different environment are almost identical. In silica saturation conditions, Icenhower et al. [36] and McGrail et al. [37] also showed that the dissolution rate of borosilicate and Na_2O-Al_2O_3-SiO_2 glass, respectively, is not affected by the presence of D_2O. The glass hydration is therefore controlled by the diffusion of water in the glass matrix through the alteration layer. This can be explained by the similarity in diffusion rates of H_2O and D_2O in glass matrix [38]. Thus, within the analytical uncertainty of 10%, the glass is hydrated in the same rate in both phases whatever their ratio in the total volume.

3.3.1.2. Analysis of hydrated glass by SEM/EDX, Raman spectroscopy and TOF-SIMS

The SEM micrograph of the glass sample #11 hydrated for 593 days at 125 °C and 95% RH in the presence of D_2O^{18} (20%) can be seen in **Fig. 10**. The alteration layer thickness is about 5 µm; it includes a 1 µm external layer of phyllosilicates and an internal 4 µm gel layer. The estimated error of thickness measurement is about 10%. the alteration gel layer thickness observed by SEM is in agreement with the measurement done by FTIR which gives a value of 4.9 ± 0.48 µm. TOF-SIMS analyses give a value of 3.8 µm for sample #11 and 2.4 µm for sample #17 hydrated for 322 days at 125 °C and 95% RH (without glass powder). For sample #17, the alteration gel layer thicknesses obtained by FTIR and SEM are 2.67 ± 0.26 and 2.5 ± 0.3 µm, respectively.

Analyses by Raman spectroscopy revealed the presence of the same phases observed in hydration experiments under water vapour at 90 and 125 °C (i.e. calcite, apatite and powellite at 90 °C; in addition to tobermorite at 125 °C).

Fig. 11a shows the TOF-SIMS profiles of boron and $^{18}O/^{16}O$ isotopic ratio for the hydrated sample at 125 °C and 95% RH in the presence of D_2O^{18} (20%) for 593 days. The depth of crater caused by sputtering is determined by combining the boron profile in the alteration layer and the abrasion rate. The latter is assumed to be the same as that obtained for the pure silica sputtering (1.33 nm s^{-1}), this assumption is further supported by FTIR and SEM analyses. C_0 corresponds to the concentration of B and $^{18}O/^{16}O$ ratio in the pristine glass and in the hydration solution, respectively. The profile of B allows distinguishing the thickness of the alteration layer and the different areas: the pristine glass where the boron concentration is maximum; the gel (between 900 and 4700 nm) and the precipitation zone (phyllosilicates) (between 0 and 900 nm). The phyllosilicates layer thickness is in good agreement with that observed by SEM (0.9−1 μm). The absence of B in the alteration layer is surprising because we have not been able to identify secondary minerals enriched in B in the phyllosilicates by the analytical techniques used in our experiments. Indeed, sodium borates are often formed in intense evaporation conditions in very alkaline salt lakes [39]. One may hypothesize that there is a water condensation on the surface of the glass monolith and a leaching of B and other elements in the Teflon holder containing the glass powder. The calculation of the elemental balance was not possible in the majority of our hydration experiments because of the high specific surface area of the glass powder compared to that of the monolith.

The isotopic profiles of $^{18}O/^{16}O$ obtained on samples #11 and #17 are illustrated in **Fig. 11**b, the sample #17 altered under the same conditions as sample #11 was used as reference. The phyllosilicates layer is characterized by the highest isotopic ratio, and the gel by an intermediate signature. The square on the origin shows a value of 0.23 for the $^{18}O/^{16}O$ ratio, corresponding to that of the hydration solution containing D_2O^{18} (20%). The incorporation of ^{18}O tracer in the alteration layer highlights two mechanisms responsible for the glass alteration. The formation of phyllosilicates on the gel surface occurs by dissolution/precipitation mechanism, while the gel is formed by a succession of hydrolysis/condensation reactions which nevertheless involves a dissolution/precipitation process far from the external solution but rather in equilibrium at a very local level (gel

porosity) where the solution does not necessarily have the same composition as the external solution (bulk). In contact with the glass, H_2O and D_2O^{18} are consumed to form Si–O^{16}–H or Si–O^{18}–D. In the presence of deuterium, a part of this process can be described by the following chemical reactions:

$\equiv Si–O^{16}–Si \equiv + D_2O^{18} \quad \equiv Si–O^{16}–D + D–^{18}O–Si \equiv$ (Hydrolysis)

$\equiv Si–O^{16}–D + D–^{18}O–Si \equiv \quad \equiv Si–O^{18}–Si \equiv + D_2O^{16}$ (Condensation)

The mechanisms show the penetration of ^{18}O in the glass and its isotopic exchange with ^{16}O of the glass. The deuterium also undergoes isotopic exchange with the hydrogen of silanol groups:

$^{16}OH–glass + D_2O^{18} \quad H_2O^{18} + {}^{16}OD–glass$

In the gel, two areas can be observed: (1) between 0.9 and 2.3 µm where the $^{18}O/^{16}O$ ratio remains constant at the value of about 0.16 and (2) between 2.3 and 4.7 µm where the $^{18}O/^{16}O$ ratio has rather a diffusion-type shape. Therefore it is possible to determine the diffusion coefficient of water in the gel according to the method described by Abdelouas et al. [5] and Bouakkaz et al. [19].

The water diffusion in the glass can be followed by measuring oxygen isotope concentrations. Thereby the isotopic profile of $^{18}O/^{16}O$ obtained on sample #11 in the area situated between 2.3 and 4.7 µm was fitted using Origin 8.6 software. A comparison of the experimental and fitting results can be seen in **Fig. 11**c. The equation is based on the second law of Fick, the latter predicts how diffusion causes the concentration to change with time and takes into account de diffusion of ^{18}O from the hydration solution in the gel which is considered a semi-infinite medium.

The second Fick law is given by:

$$\frac{\partial C}{\partial x} = D\frac{\partial^2 C}{\partial t^2} \quad (4)$$

Where C is the concentration of the component in the condensed water film in g m^{-3}, x is the distance in meters, D is the diffusion coefficient in m^2 s^{-1} and t is the time in seconds.

The solution of this equation is:

$$C(x,t) = \frac{1}{\sqrt{2\pi\sigma^2}} exp \frac{-(x)^2}{2\sigma^2} \quad \text{With } \sigma = \sqrt{2Dt} \quad (5)$$

This gives the equation:

$$C(x,t) = A \times exp \frac{-(X-d)^2}{4D \times t} \quad \text{With } A = \frac{1}{\sqrt{2\pi\sigma^2}} \quad (6)$$

A is temperature-independent pre-exponential in $m^2\ s^{-1}$ (the height of the curve's peak), *d* is the position of the centre of the peak, *D* is the diffusion coefficient and *t* is the time of the experiment. The obtained value of D_2O^{18} apparent diffusion coefficient from TOF-SIMS profile is about $2.3 \times 10^{-19}\ m^2\ s^{-1}$, it is in agreement with the value obtained previously from FTIR measurements ($5.3 \times 10^{-19}\ m^2\ s^{-1}$).

3.4. Alteration in solution of hydrated samples

3.4.1. Evolution of pH

The pH measured for each experiment increases rapidly from the first day of alteration (**Fig. 12**), it ranges from 6.7 to 7.7 for the sample #09 (pre-hydrated at 35 °C and 95% RH for 654 days) and from 6.7 to 8.4 for the sample #08 (pre-hydrated at 125 °C and 95% RH for 654 days). The pH continues to increase before stabilizing around 29 days. The leaching solution of the non-hydrated glass monolith (Blank) show the lower pH value (6.9 after one day and it stabilizes after 29 days). The monoliths previously hydrated at high temperatures and relative humidity values show the highest pH values. The rapid increase in pH for solutions containing pre-hydrated monoliths is due to the rapid release of glass alkaline elements present in the alteration gel. For the solution containing the non-hydrated glass sample, the pH increases slightly at the beginning of the experiment indicating a low dissolution of the pristine glass compared to pre-hydrated glass.

3.4.2. Evolution of elemental release

Fig. 13a and b illustrate the evolution the normalized mass loss of the glass tracer elements (*NL*, $g\ m^{-2}$) versus time for samples hydrated for 766 days under 95% RH and at 35 and 125 °C respectively, and then leached in COx water at 50 °C for 78 days. A glass tracer can be defined as an element leached from the glass and totally remains in solution (no precipitation in the alteration layer). Thus, it is used to calculate the glass dissolution rate. Data are compared to a pristine glass sample. For the latest, the release of glass tracers is congruent

from the first contact with leaching solution. It is also the case until the end of the experiment except for Mo, which showed a slowdown release from 11 days. This difference was also observed during the glass alteration in dynamic mode under Si-rich COx water [19] and was attributed to the incorporation of Mo in the alteration layer. For pre-hydrated monoliths, incongruent release of glass tracers was observed from the first instants of glass leaching. This incongruence is most significant for samples hydrated at high temperature and RH values. As seen in **Fig. 13**b, the pre-hydrated monolith at 125 °C and 95% RH releases instantly the glass components compared to the pristine glass monolith. The release of B and Li at the end of the experiment is 10 times higher than that observed for the pristine glass. An increase of a factor of 10 in the release of tracers was also observed by Neeway et al [4]. for the alteration of pre-hydrated SON68 glass at 125 °C and 92% RH in DI water. For SRL 211 glass, an increase of a factor of 3 was observed and was assigned to an increase in the surface area of the hydrated glass [40]. It must also be noted that the boron which was depleted in the layer represents the lowest NL value (**Fig. 13**b). As was previously suggested, this may be due to a leaching of B due to water condensation on glass monoliths during hydration experiments.

It is difficult in the present study to attribute this behaviour to a simple increase in the surface area, or to a rapid dissolution of the gel formed during hydration and thus its nature which may be relatively fragile. The rapid release of glass tracers in solution is therefore a result of a more instantaneous dissolution of fast-dissolving rich phases, such as Cs- and Mo-rich phases, incorporated in the gel and/or surface precipitates in which they are retained as salt form. This hypothesis is reinforced by the behaviour of Mo and a lesser extent of Cs in **Fig. 13**b. Mo present in the alteration layer as powellite phase shows the most elevated normalized mass loss value. Cs for its part is renowned to have a faculty to be incorporated into solid phases, particularly the clays [41,42]. In addition, after the instant release, the normalized mass losses of elements seem to follow the same patterns suggesting that the long term alteration is controlled by the underlying glass.

The evolution with time of the normalized mass loss (*NL*, g m^{-2}) of glass tracers for all samples hydrated under various conditions and then leached in COx water for 78 days at 50 °C is shown in **Fig. 14**a–d. B and Li behave almost in the same manner for all glass monoliths (**Fig. 14**a and b). For sample #11 (hydrated at 125 °C and 95% RH in the presence of D_2O^{18}, 20%), the release of B and Li is slightly slowed during the first days leaching compared to

samples #08 and #17 hydrated in the same conditions in pure water vapour. Indeed, the normalized mass losses of the B and Li for samples #08, #11 and #17 tend toward the same value after around 60 days of alteration. Similarly, the alteration of sample #10 (hydrated at 90 °C and 95% RH in the presence of D_2O^{18}, 20%) is slowed in the first 29 days of alteration. This observation can be explained by the difference in nature between the gels formed in the presence and in the absence of deuterium. In fact, the substitution of 20% H_2O by D_2O^{18} produced less O–H bonds whose breaking produces protons (H^+). These last are responsible for the ion exchange with the cations Na+, Li+... to maintain electrical neutrality, the cations therefore diffuse freely in the solution. In addition, the polycondensation reaction of silanes hydrolysed by D_2O^{18} is carried out more easily than those hydrolysed by H_2O [43]. This phenomenon allows a rapid reconstitution of (≡Si–O–Si ≡) network. Thus, the morphology of the gel formed in the presence of deuterium is expected to be more compact and less hydrated than that formed in the presence of pure water. This leads to slower dissolution of rich phases instead incorporated in the gel.

This hypothesis is further supported by the evolution of NL Cs and NL Mo (**Fig. 14**c and d) for samples #10 and #11 (hydrated in the presence of deuterium). Unlike B and Li, the release of Cs and Mo during the first contact with leaching solution is not slowed compared to samples hydrated in the presence of pure water at the same conditions. This does not seem to be enhanced by the dissolution of (Cs, Mo)-rich phases incorporated in the gel layer that differs depending on hydration atmosphere but rather to the external precipitates rich in these elements (phyllosilicates). Also, it can be noted that NL Mo for samples hydrated at 125 °C (samples #08, #11 and #17) are significantly higher than those for the other samples. This can be attributed to the formation of the large quantity of powellite at 125 °C.

3.4.3. Effect of hydration temperature and relative humidity on the glass alteration in COx water at 50 °C

Fig. 15 shows the evolution of the normalized mass loss of boron (*NLB*, g m^{-2}) as a function of time for leaching experiments in COx water of pre-hydrated SON68 glass monoliths at: different temperatures and 95% RH (a); different relative humidities and 90 °C (b); 95% RH and 90 °C (c) and 125 °C (d) in H_2O and D_2O^{18} (20%). The same behaviour was observed for all tracers. As described above, the pre-hydrated monoliths at high temperatures release more elements than those pre-hydrated at low temperatures (**Fig. 15**a), due to the dissolution of the hydration layer, which is thicker at high temperatures. The same effect is observed for glass

hydrated at 92 and 98% RH. As in the case of temperature, the normalized mass loss increases with time and relative humidity (**Fig. 15**b). The same was observed for glass hydrated at 50 °C. The effect of the hydration time can also be seen in **Fig. 15**b, where the normalized mass loss increases for glass hydrated at 95% RH (sample #06) compared to that hydrated at 98% RH (sample #12). Indeed, before putting back in COx water, sample #06 was hydrated for 652 days while sample #12 was hydrated for 482 days. In **Fig. 15**c and d, the release of boron in solution during the first days of alteration is slowed for pre-hydrated samples in presence of deuterium, indicating the difference in nature between the gels formed in different atmospheres.

Conclusion

We investigated the vapour hydration of the SON68 glass under different conditions of temperature (35–125 °C) and relative humidity (92–99.9%) relevant to high-level waste geological disposal in France. The glass hydration increased with increasing time, temperature and relative humidity. Measurements of hydration thicknesses using 3 different techniques, SEM, FTIR and TOF-SIMS, allowed calculating a glass hydration activation between 34 (±4) and 68 kJ mol^{-1}, consistent with a diffusion and chemical reaction processes. The water diffusion coefficient at 90 °C and 95% RH, 7.5×10^{-20} m^2 s^{-1}, is 350 times higher than that reported by Ferrand et al. [22] (2×10^{-22} m^2 s^{-1}) for the SON68 glass altered at 90 °C in a Si-saturated (240 ppm) synthetic solution.

In the presence of D_2O^{18} (20 %), the incorporation of ^{18}O in the alteration layer revealed two mechanisms responsible for the glass alteration. The formation of phyllosilicates occurs by a dissolution/ precipitation process from the supersaturation of the bulk solution while the gel is formed by a succession of very local hydrolysis/condensation reactions (away from the bulk solution). The apparent diffusion coefficient of D_2O^{18} is about 2.3×10^{-19} m^2 s^{-1}.

The alteration in COx water of pre-hydrated glass samples showed the instantaneous release of glass tracer elements, much faster than for the non-hydrated glass sample. The phenomenon is due to an instantaneous dissolution of fast-dissolving phases (e.g. salts) incorporated in the hydrated layer.

Finally, in the context of geological disposal of HLW it is important to evaluate the water under-saturation period to better assess the radionuclides release in the groundwater contacting the hydrated glass.

Acknowledgement

The authors are grateful to Andra for the partial financial support of this work. They would also like to thank Nicolas Stephant from the Institut des Matériaux de Nantes Jean Rouxel (Nantes, France) for his help with SEM analyses, and Yassine El Mendili from SUBATECH for his help with Raman analyses.

References

[1] J.K. Bates, M.J. Steindler, B. Tani, F.J. Purcell, The hydration alteration of a commercial nuclear waste glass, Chem. Geol. 51 (1985) 79–87.

[2] T.A. Abrajano Jr, J.K. Bates, C.D. Byers, Aqueous Corrosion of Natural Nuclear Waste Glasses. I. Comparative Rates of Hydration in Liquid and Vapor Environments at Elevated Temperatures, J. Non-Cryst. Solids. 84 (1986) 251–257.

[3] J.K. Bates, W.L. Ebert, T.J. Gerding, Vapor hydration and subsequent leaching of transuranic-containing SRL and WV glasses, in: Proceedings of the International High-Level Radioactive Waste Management Topical Meeting, American Nuclear Society, Las Vgas, NV, April 8–12, 1990, p. 1095.

[4] J. Neeway, A. Abdelouas, B. Grambow, S. Schumacher, C. Martin, M. Kogawa, S. Utsunomiya, S. Gin, P. Frugier, The French SON68 Glass Vapor Hydration under Different Atmospheres, J. Non-Cryst. Solids. 358 (2012) 2894–2905.

[5] A. Abdelouas, Y. EL Mendili, A. Aït Chaou, G. Karakurt, C. Hartnack, J.F. Bardeau, T. Saito, H. Matsuzaki, A Preliminary Investigation of the ISG Glass Vapor Hydration, Int. J. Appl. Glass. Sci. 4 (2013) 307–316.

[6] A. Aït Chaou, A. Abdelouas, Y. El Mendili, R. Bouakkaz, S. Utsunomiya, C. Martin, X. Bourbon, Vapor hydration of a simulated borosilicate nuclear waste glass in unsaturated conditions at 50 °C and 90 °C, RSC. Adv. 5 (2015) 64538–64549.

[7] J.J. Mazer, C.M. Stevenson, W.L. Ebert, J.K. Bates, The experimental hydration of obsidian as a function of relative humidity and temperature, American Antiquity. 56 (1991) 504–513.

[8] K.L.Hull, Reasserting the utility of obsidian hydration dating: a temperature-dependent empirical approach to practical temporal resolution with archaeological obsidians, J. Archaeol. Sci. 28 (2001) 1025–1040.

[9] L.R. Riciputi, J.M. Elam, L.M. Anovitz, D.R. Cole, Obsidian Diffusion Dating by Secondary Ion Mass Spectrometry: A Test using Results from Mound 65, Chalco, Mexico, J. Arch. Sci. 29 (2002) 1055–1075.

[10] L.M. Anovitz, D.R. Cole, M. Fayek, Mechanisms of rhyolitic glass hydration below the glass transition, Am. Mineral. 93 (2008) 1166–1178.

[11] N. Laskaris, A. Sampson, F. Mavridis, I. Liritzis, Late Pleistocene/Early Holocene seafaring in the Aegean: new obsidian hydration dates with the SIMS-SS method, J. Arch. Sci. 38 (2011) 2475–2479.

[12] W.L. Ebert, R.F. Hoburg, J.K. Bates, The sorption of water on obsidian and a nuclear waste glass, Phys. Chem. Glasses. 32 (1990) 133–137.

[13] K.S. Pitzer, D.J. Bradley, Thermodynamics of High Temperature Brines, in: Lawrence Berkeley Lab., Univ. California, Berkeley, CA, USA, 1979, p. 40.

[14] W.L. Gong, L.M. Wang, R.C. Ewing, E. Vernaz, J.K. Bates, W.L. Ebert, Analytical electron microscopy study of surface layers formed on the French SON68 nuclear waste glass during vapor hydration at 200 °C, J. Nucl. Mater. 254 (1998) 249–265.

[15] P. Van Iseghem, B. Grambow, The long-term corrosion and modelling of two simulated Belgian reference high-level waste glasses, MRS Online Proc. Libr. 112 (1987) 631–640.

[16] D.M. Strachan, T.L. Croak, Compositional effects on long-term dissolution of borosilicate glass, J. Non-Cryst. Solids. 272 (2000) 22–33.

[17] S. Gin, X. Beaudoux, F. Angéli, C. Jégou, N. Godon, Effect of composition on the short-term and long-term dissolution rates of ten borosilicate glasses of increasing complexity from 3 to 30 oxides, J. Non-Cryst. Solids. 358 (2012) 2559–2570.

[18] A. Aït Chaou, A. Abdelouas, Y. EL Mendili, R. Bouakkaz, C. Martin, The French SON68 glass vapor hydration under different Atmospheres, Proc. Mater. Sci. 7 (2014) 179–185.

[19] R. Bouakkaz, A. Abdelouas, Y. El Mendili, B. Grambow, S. Gin, SON68 glass alteration under Si-rich solutions at low temperature (35–90 _C): kinetics, secondary phases and isotopic exchange studies, RSC. Adv. 5 (2016) 64538–64549.

[20] ANDRA, Dossier 2005 Argile, Tome, Phenomenological Evolution of a Geological Repository, in: ANDRA Report C.RP.ADS.04.0025, 2005, pp. 1–525.

[21] E.C. Gaucher, C. Lerouge, P. Blanc and C. Tournassat, Caractérisation géochimique des forages PAC et nouvelles modélisations THERMOAR. BRGM/RP–5446–FR, 2007.

[22] K. Ferrand, A. Abdelouas, B. Grambow, Water diffusion in the simulated French nuclear waste glass SON68 contacting silica rich solutions: Experimental and modeling, J. Nucl. Mater. 355 (2006) 54–67.

[23] K.M. Davis, M. Tomozawa, An infrared spectroscopic study of water-related species in silica glasses, J. Non-Cryst. Solids, 201 (1996) 177–198.

[24] J.J. Neeway, The alteration of the SON68 reference waste glass in silica saturated conditions and in the presence of water vapour, PhD thesis, University of Nantes (France), 2011.

[25] J. Crank, The mathematics of diffusion, in: Oxford University Press, New York, 1956, p. 12–15.

[26] T. Chave, P. Frugier, A. Ayral, S. Gin, Solid state diffusion during nuclear glass residual alteration in solution, J. Nucl. Mater. 362 (2007) 466–473.

[27] D. Rébiscoul, F. Bruguier, V. Magnin, S. Gin, Impact of soda-lime borosilicate glass composition on water penetration and water structure at the first time of alteration, J. Non-Cryst. Solids.358 (2012) 2951–2960.

[28] A. Abdelouas, J.-L. Crovisier, W. Lutze, B. Grambow, J.-C. Dran, R. Müller, Surface layers on a borosilicate nuclear waste glass corroded in $MgCl_2$ solution, J. Nucl. Mater. 240 (1997) 100–111.

[29] D. Bosback, T. Rabung, F. Brandt, T. Fanghanel, Trivalent actinide coprecipitation with powellite (CaMoO4): secondary solid solution formation during HLW borosilicate-glass dissolution, Radiochim. Acta 92 (2004) 639–643.

[30] J.C. Elliott, Structure and chemistry of the apatites and other calcium orthophosphates. In: Studies in Inorganic Chemistry., 1994, 18. Elsevier, p. 389.

[31] P. Mandaliev, T. Stumpf, J. Tits, R. Dähn, C. Walther, E. Wieland, Uptake of Eu(III) by 11 Å tobermorite and xonotlite: a TRLFS and EXAFS study, Geochim. Cosmochim. Acta 75 (2011) 2017–2029.

[32] G. Jakli, The H_2O–D_2O solvent isotope effects on the molar volumes of alkali-chloride solutions at T = (288.15, 298.15, and 308.15) K, J. Chem. Thermodynamics. 39 (2007) 1589–1600.

[33] M. Kakiuchi, Distribution of isotopic water molecules, H_2O, HDO and D_2O, in vapour and liquid phases in pure xater and aqueous solutions systems, Geochim. Cosmochim. Acta. 64 (2000) 1485–1492.

[34] P. Gupta, A.C. Dillon, A.S. Bracker, S.M. George, FTIR studies of H_2O and D_2O decomposition on porous silicon surfaces, Surf. Sci. 245 (1991) 360–372.

[35] L.M. Anovitz, D.R. Cole, L.R. Riciputi, Low-temperature isotopic exchange in obsidian: Implications for diffusive mechanisms, Geochim. Cosmochim. Acta. 73 (2009) 3795–3806.

[36] J.P. Icenhower, E.M. Pierce and B.P. McGrail, The Impact of Na—H^+ Exchange on Long-Term Borosilicate Glass Corrosion: Experiments and Field Observations (PNNL-SA-64130). United States, 2009.

[37] B.P. McGrail, J.P. Icenhower, D.K. Shuh, P. Liu, J.G. Darab, D.R. Baer, S. Thevuthasen, V. Shutthanandan, M.H. Engelhard, C.H. Booth, P. Nachimuthu, The structure of Na_2O–Al_2O_3–SiO_2 glass: impact on sodium ion exchange in H_2O and D_2O, J. Non-Cryst. Solids. 296 (2001) 10–26.

[38] L.M. Anovitz, D.R. Cole, M. Fayek, Mechanisms of rhyolitic glass hydration below the glass transition Am. Mineral. 93 (2008) 1166–1178.

[39] J. García-Veigas, C. Helvac, Mineralogy and sedimentology of the Miocene Göcenoluk borate deposit, Kırka district, western Anatolia, Turkey, Sedim. Geol. 290 (2013) 85–96.

[40] J.K. Bates, L.J. Jardine, M.J. Steindler, Hydration aging of nuclear waste glass, Science 218 (1982) 51–54.

[41] G. Montavon, E. Alhajji, B. Grambow, Study of the interaction of Ni^{2+} and Cs^+ on MX-80 bentonite; effect of compaction using the "capillary method". Environ. Sci. Technol. 40 (2006) 4672–4679.

[42] A.A. Hazotte, O. Peron, A. Abdelouas, G. Montavon, T. Lebeau, Microbial mobilization of cesium from illite: The role of organic acids and siderophores, Chem. Geol. 428 (2016) 428, 8–14.

[43] Z. Zhiyi, X. Gaozhi, P. Guang, Z. Pinqing and Z. Ming, Application of deuterium oxide in producing silicon containing and metal containing materials, In (patent application), Pub. N 0.2 US 2001/0047665 A1. Dec. 6, 2001.

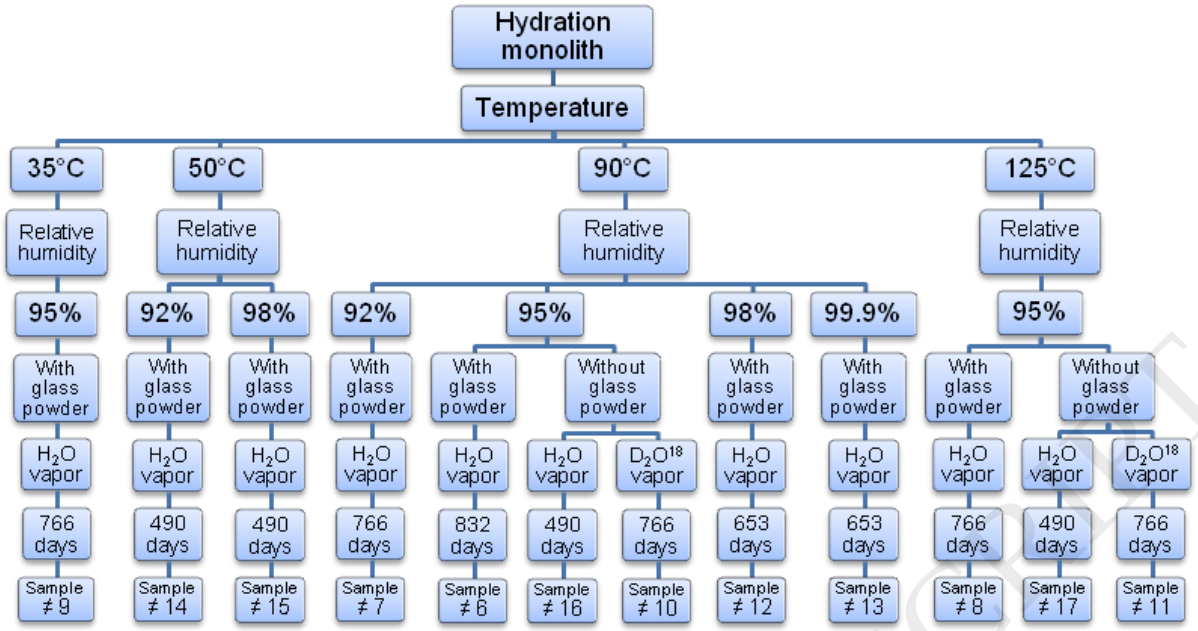

Fig. 1. Flowchart summarizing all the hydration experiments carried out in this work with the operational conditions. The glass monoliths in the experiments 10 and 11 are hydrated in the presence of D_2O^{18} (20%). In experiments 16 and 17, the glass powder was not added in order to compare with hydration experiments in the presence of D_2O^{18} (experiments 10 and 11, respectively).

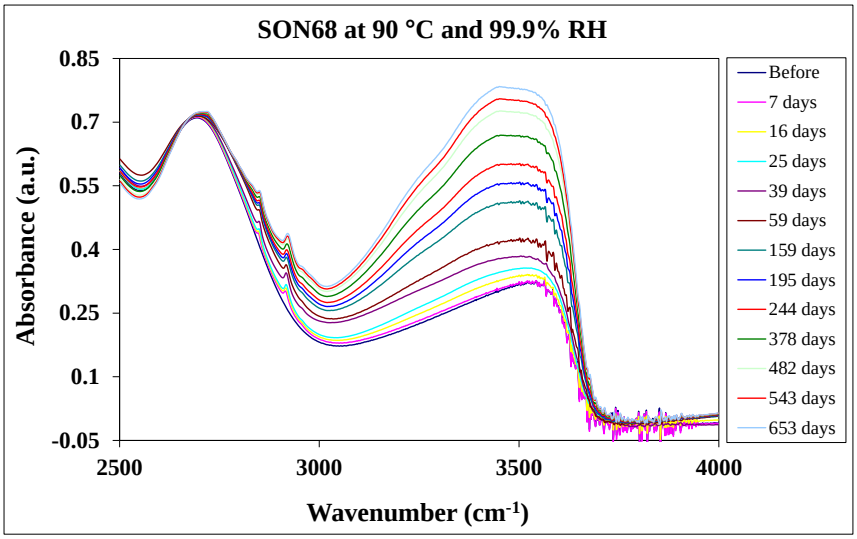

Fig. 2. Evolution with time of FTIR spectrum for SON68 glass sample hydrated at 90 °C and 99.9% RH.

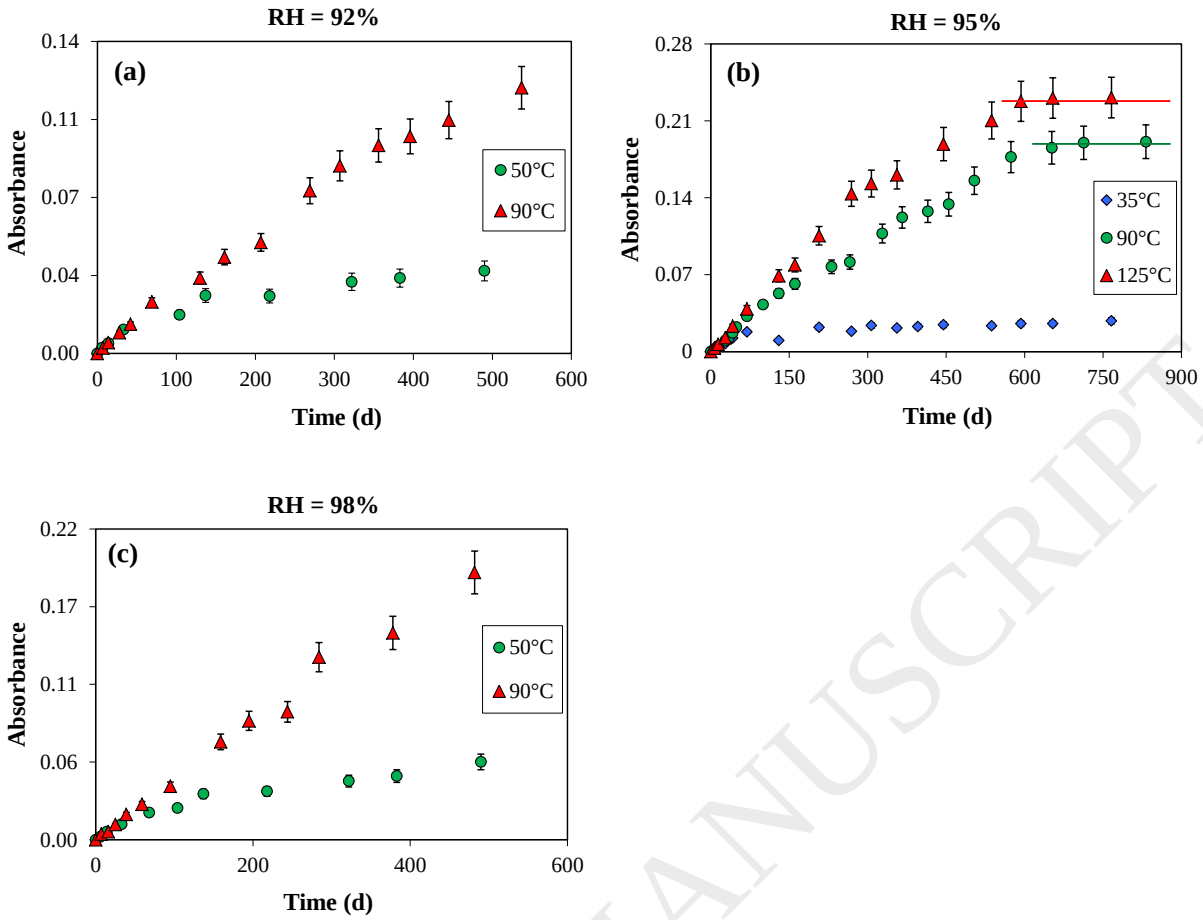

Fig. 3. The growth of the absorbance of the SiOH peak at 3595 cm^{-1} as a function of time and temperature for SON68 glass hydrated under relative humidities of 92% (a), 95% (b) and 98% (c). Errors are less than 10%.

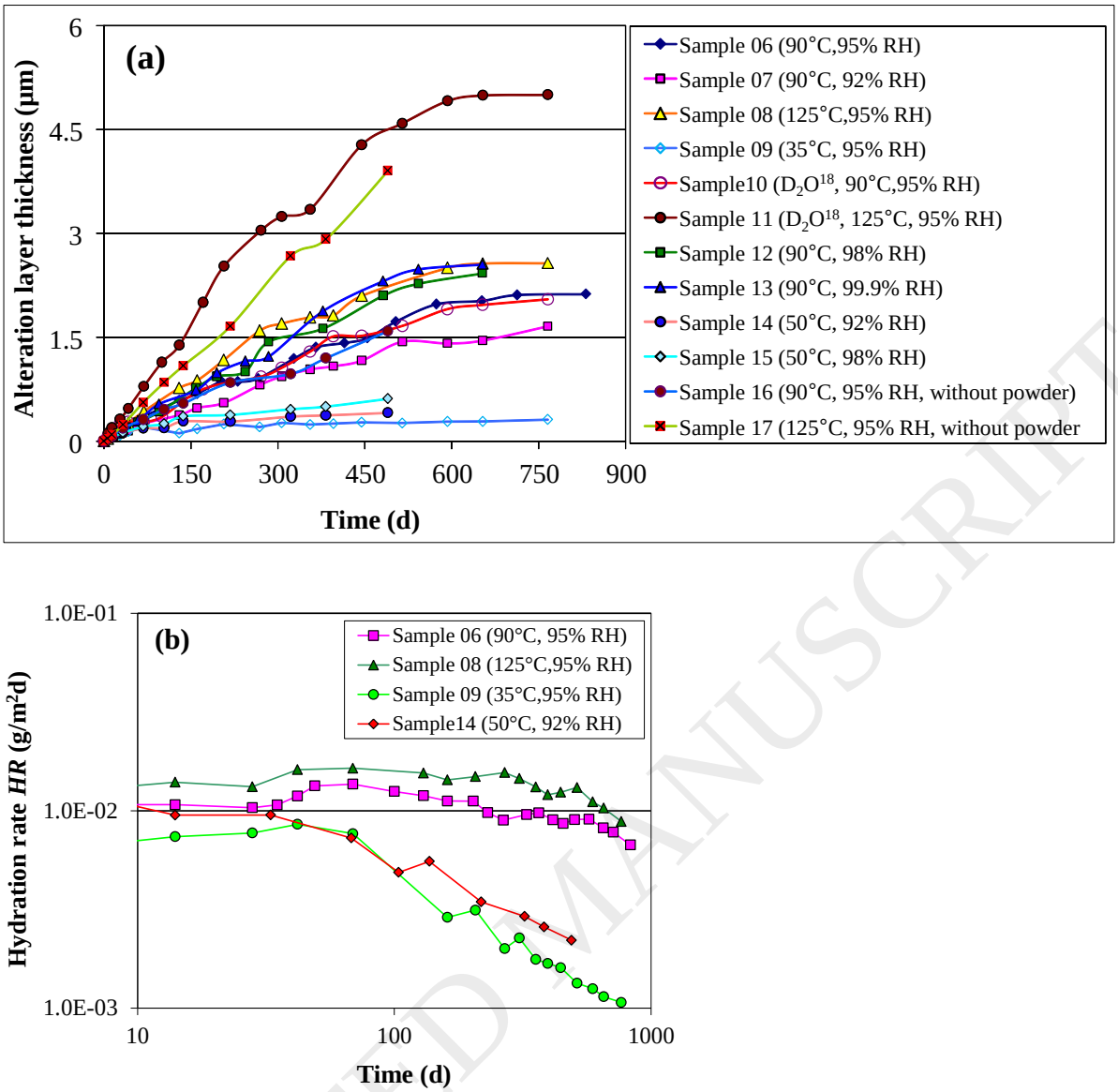

Fig. 4. (a) Evolution of the alteration layer thickness over time for each SON68 glass sample. (b) Evolution of the hydration rate HR (g m^{-2} d^{-1}) as a function of time for different temperatures and relative humidity values.

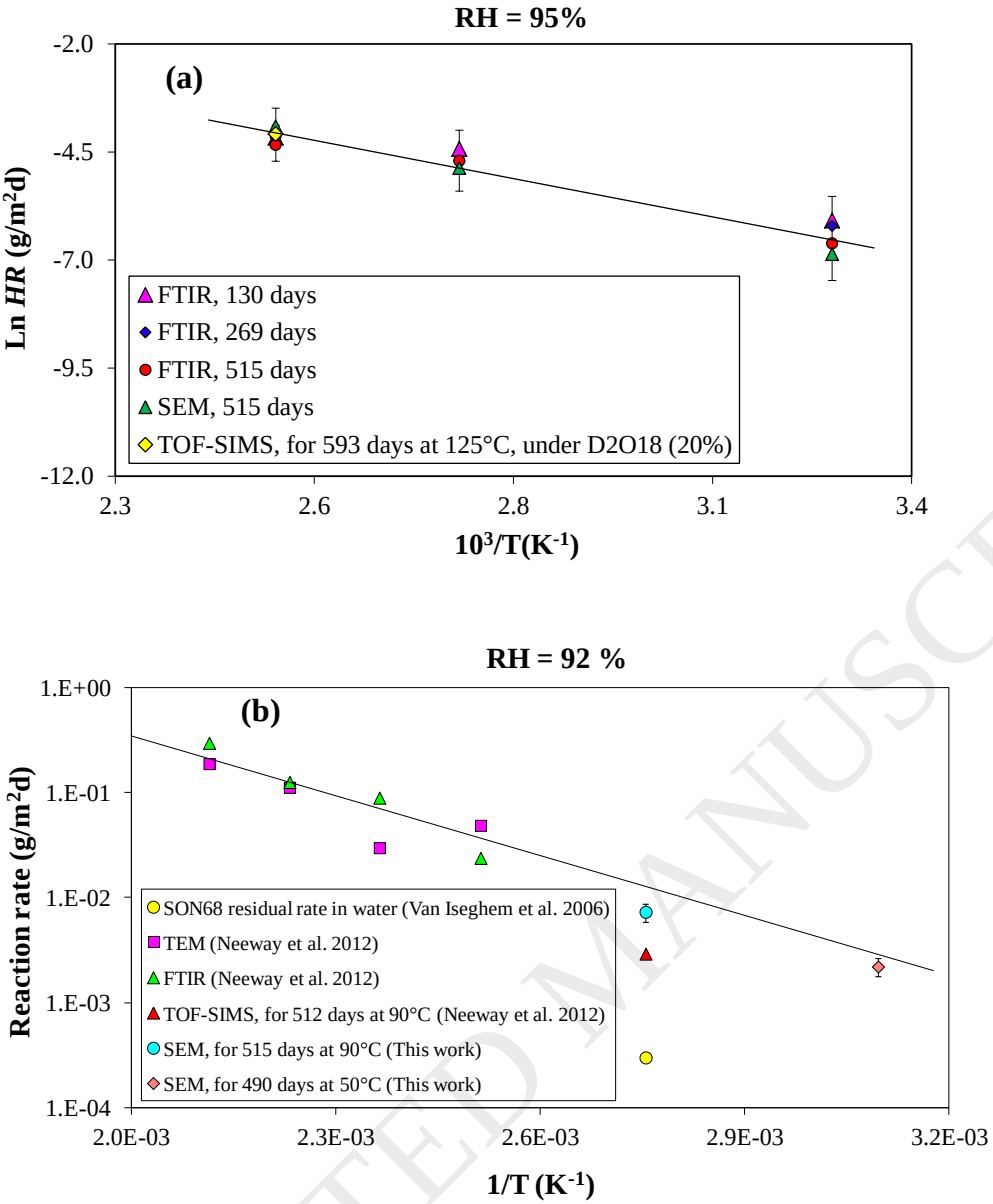

Fig. 5. (a) The logarithm of the glass hydration rate versus the inverse of the temperature; the rates are calculated from the alteration layer thicknesses measured by FTIR, SEM and SIMS techniques for samples hydrated under 95% RH. (b) An Arrhenius plot of the SON68 glass hydration at various temperatures for 92% RH measured using TEM and FTIR for the thickness of the altered layer [4]; results are compared to the present work and show good agreement.

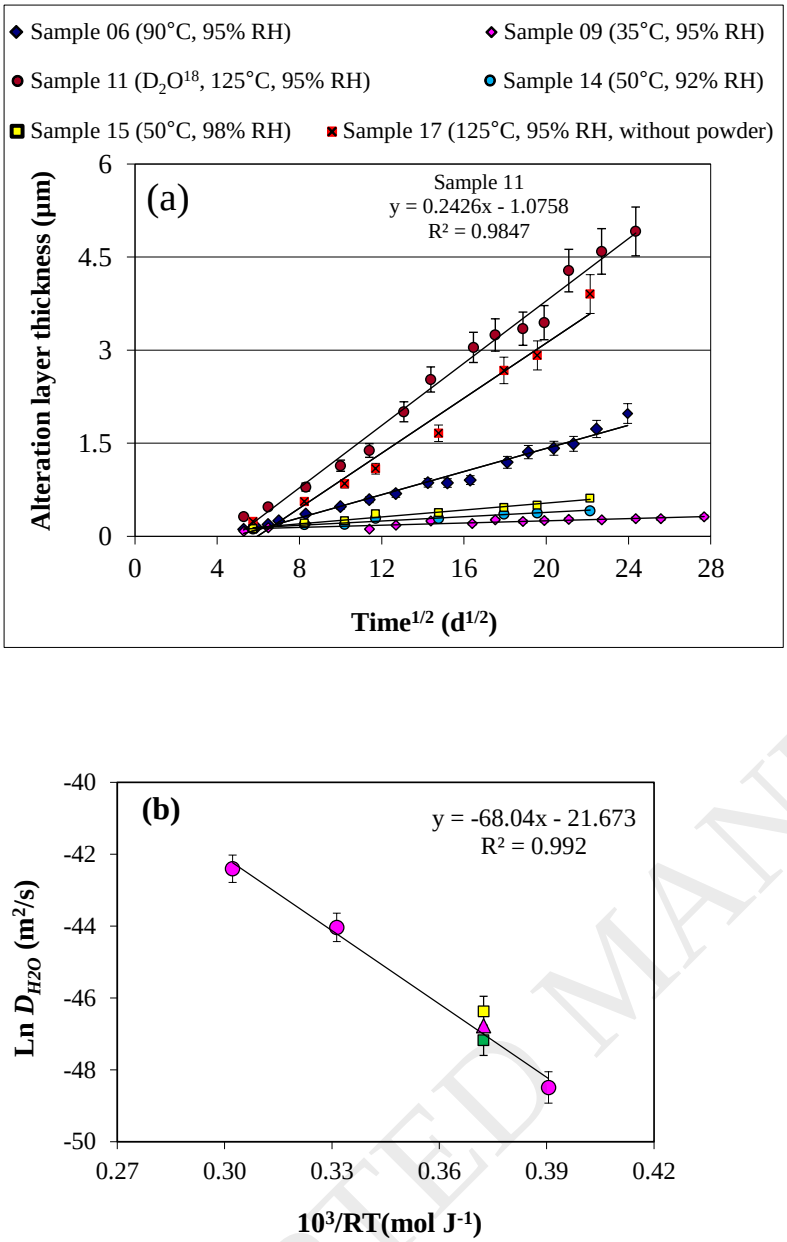

Fig. 6. (a) Evolution of the alteration layer thickness versus square root of time. (b) Logarithm of the water diffusion coefficient D_{H2O} versus the inverse temperature, data are obtained from samples #06; #09; #17 and the average of sample #14 and #15 (green and yellow square, respectively) listed in **Table 5**.

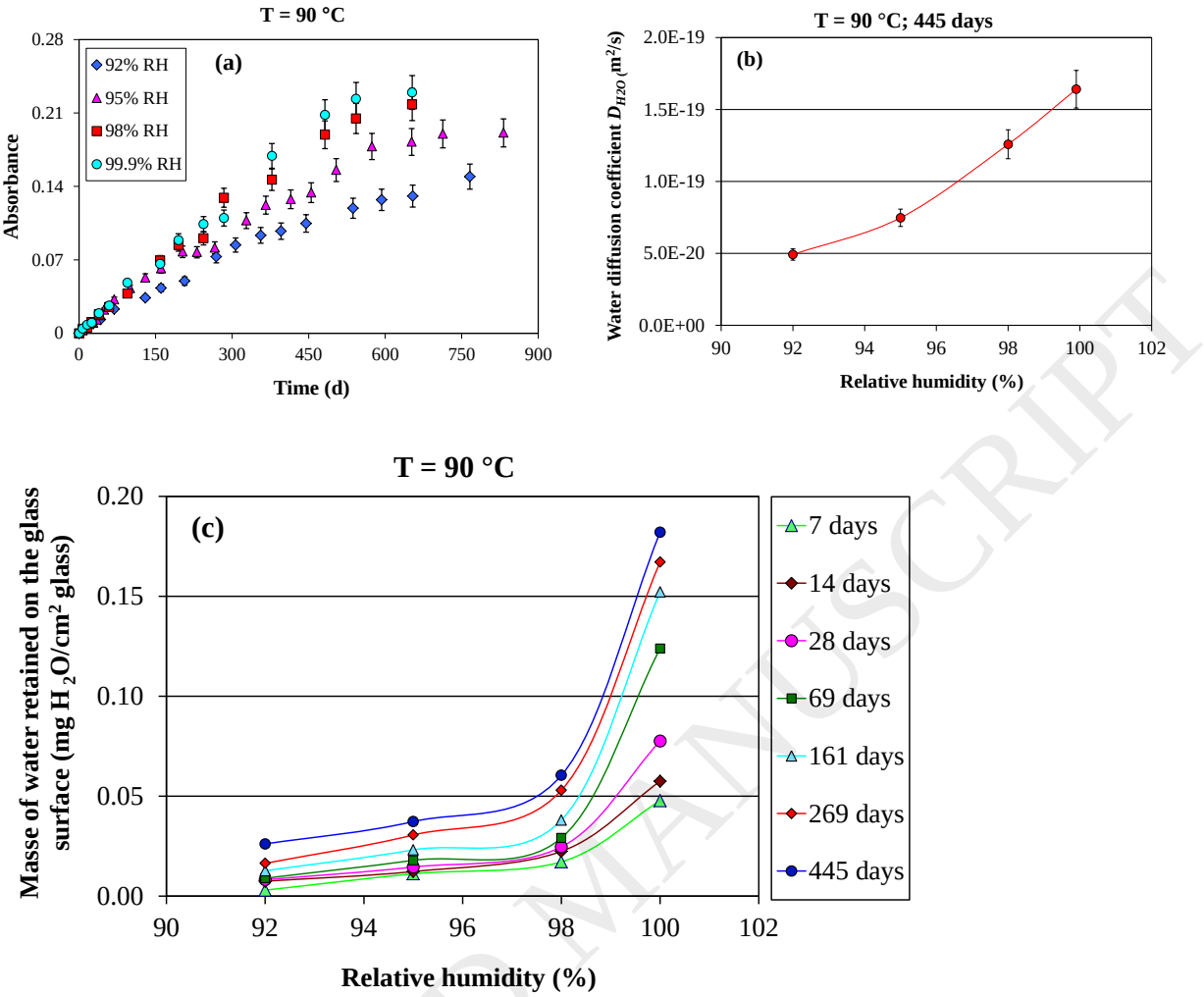

Fig. 7. (a) The growth of the absorbance of the SiOH peak at 3595 cm^{-1} as a function of time and relative humidity for SON68 glass hydrated at 90 °C; errors stay under 10%. (b) Evolution of the water diffusion coefficient D_{H2O} versus RH for samples hydrated at 90 °C for 445 days. (c) Evolution of the mass of water retained on the glass samples (mg_{H2O}/cm^2 glass) hydrated at 90 °C as a function of RH for different time intervals.

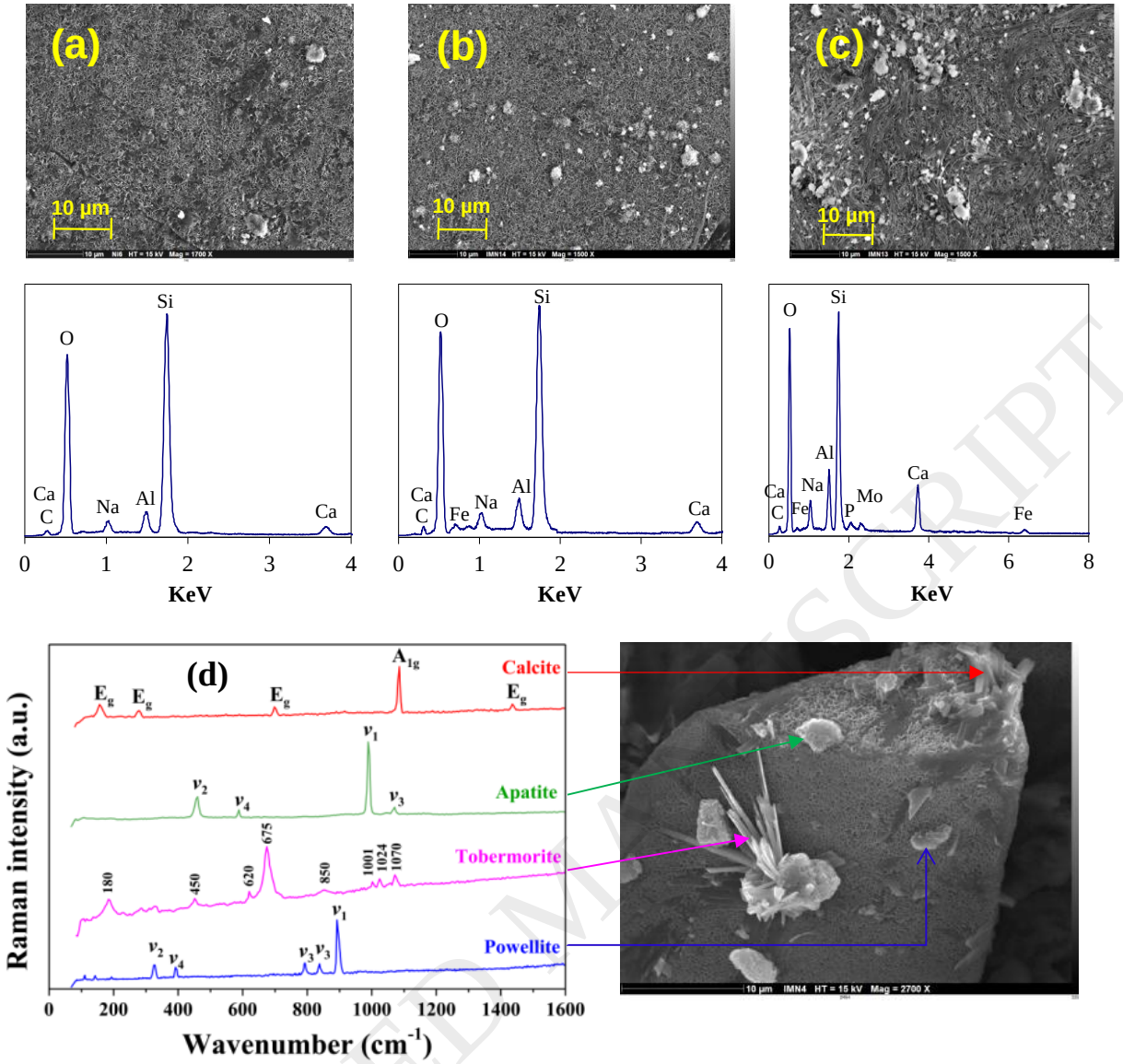

Fig. 8. SEM micrographs with the corresponding EDX spectra of the SON68 glass monoliths hydrated at: (a) 35 °C and 95% RH to 654 days; (b) 50 °C and 98% RH to 490 days; (c) 90 °C and 95% RH to 652 days. (d) SON68 glass powder hydrated to 593 days at 125 °C and 95% RH, the different precipitates are indicated by the corresponding Raman spectrum.

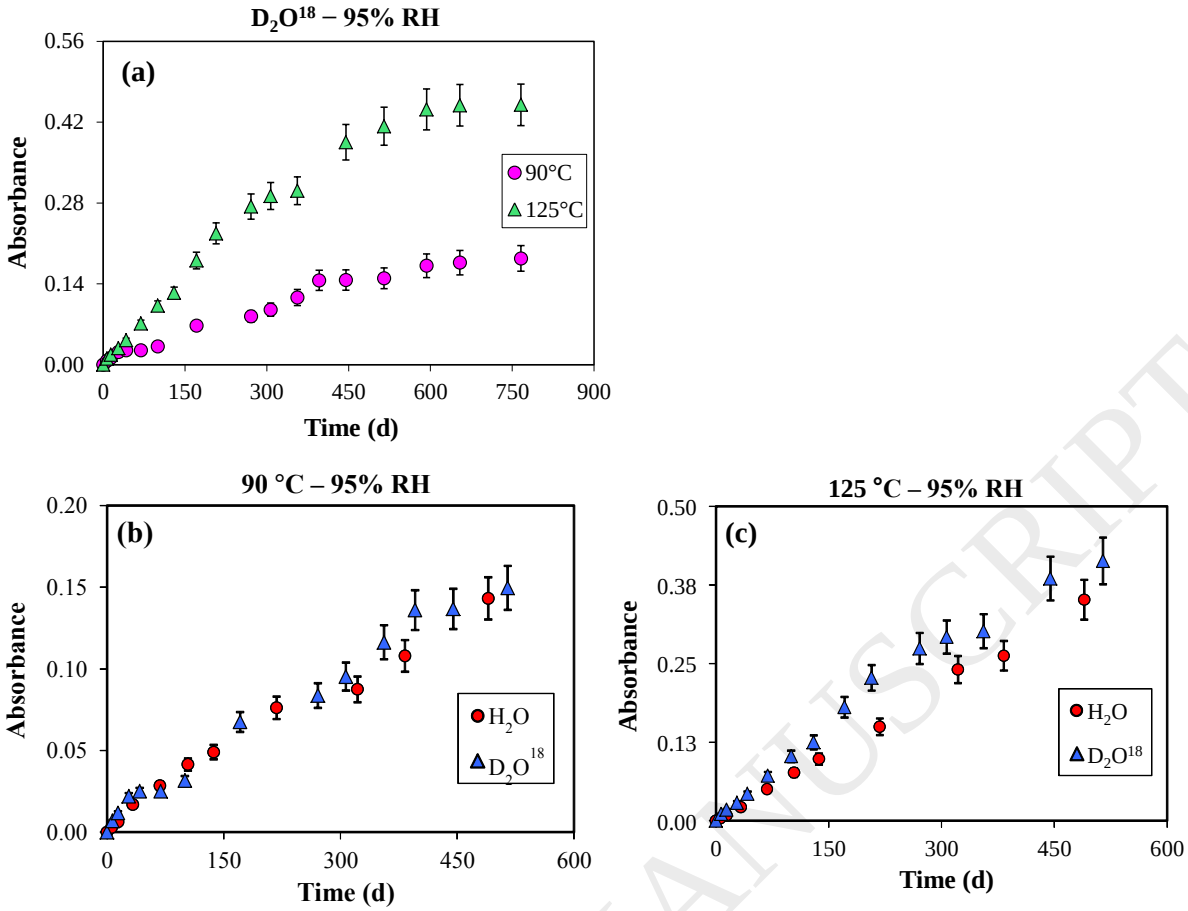

Fig. 9. The growth of the absorbance of the peak at 3595 cm^{-1} as a function of time for SON68 glass hydrated under 95% RH at: (a) 90 and 125 °C and in the presence of a saline solution containing D_2O^{18} (20%); (b) 90 °C and (c) 125 °C in vapour phase of pure water and in the presence of D_2O^{18} (20%). Errors stay under 10%.

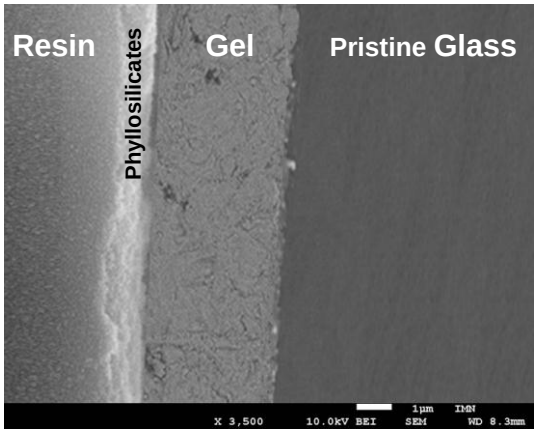

Fig. 10. Profile of the layer formed after the hydration of the sample #11 for 593 days at 125 °C and 95% RH in the presence of saline solution containing D_2O^{18} (20%). The error is about 10%.

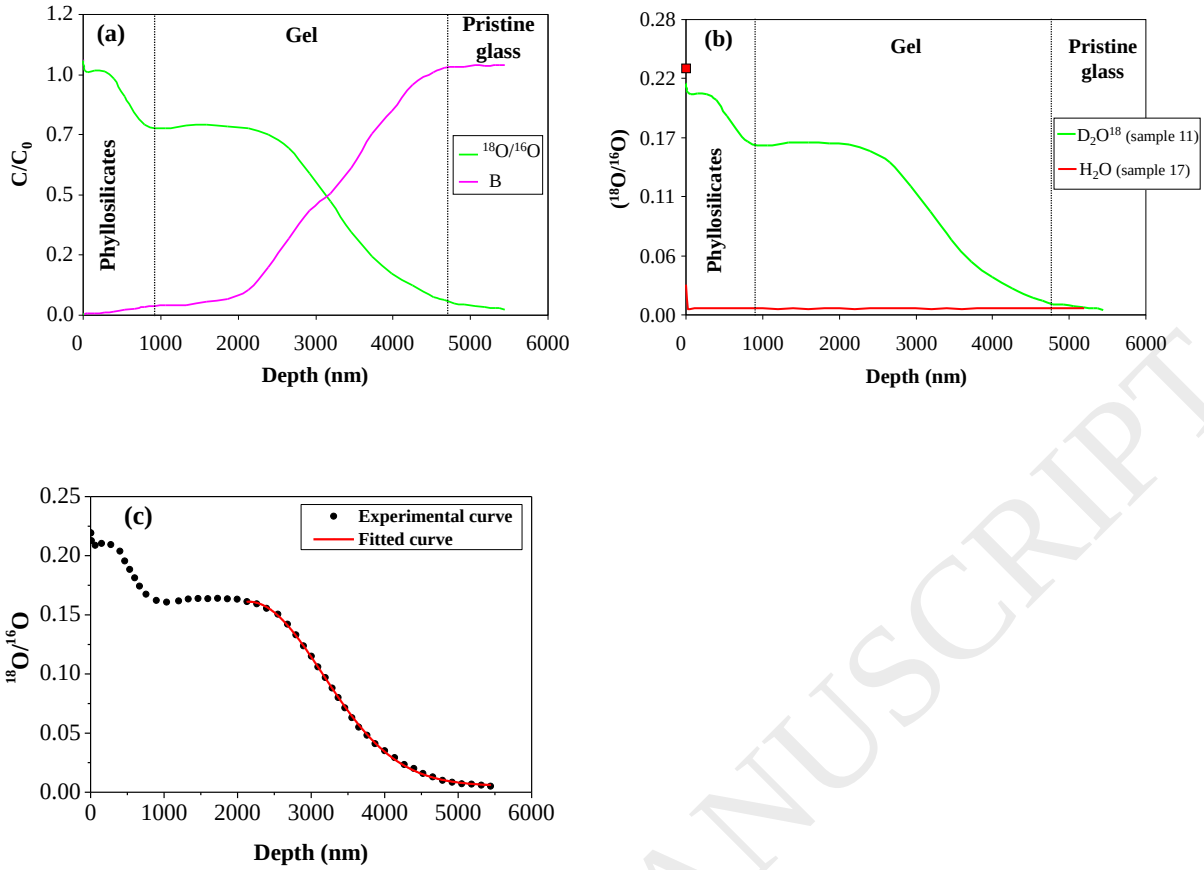

Fig. 11. (a) TOF-SIMS profiles of B and $^{18}O/^{16}O$ isotopic ratio for SON68 glass hydrated to 593 days at 125 °C and 95% RH in the presence of D_2O^{18} (20%) (sample #11). (b) Profile of $^{18}O/^{16}O$ isotopic ratio for sample #11 compared to sample #17 (hydrated to 322 days at 125 °C and 95% RH in the pure water); the square on the origin presents the value of the $^{18}O/^{16}O$ ratio (0.23) for the hydration solution containing D_2O^{18} (20%). (b) Modelling of oxygen diffusion in the gel for the hydration experiment of sample #11.

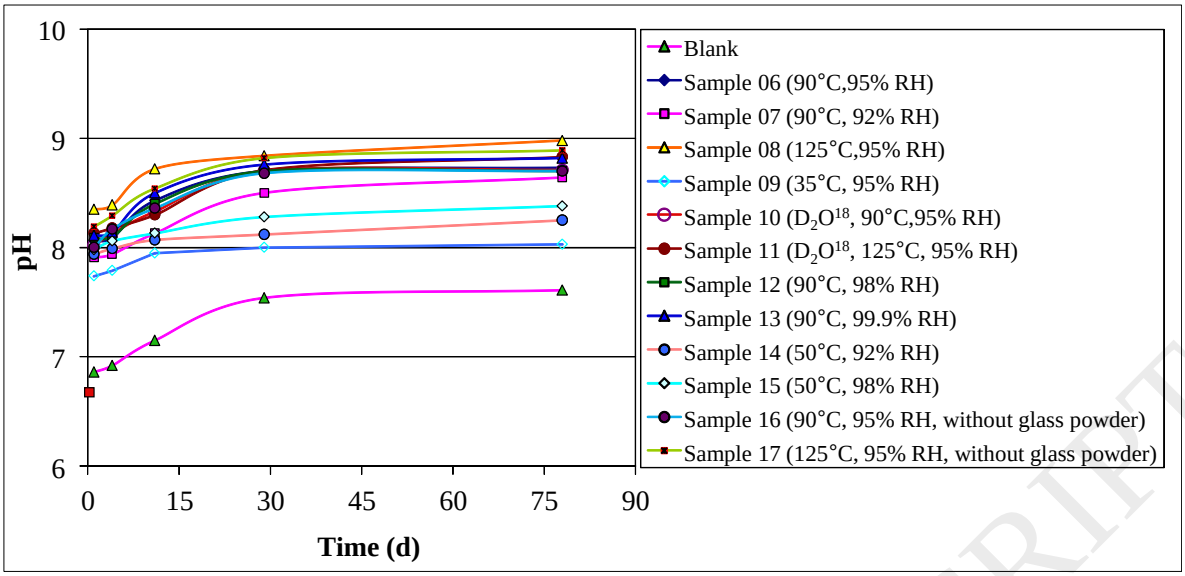

Fig. 12. Evolution with time of pH in alteration solutions containing the glass monoliths pre-hydrated under various conditions. The square on the origin presents the initial value of pH in the alteration solution (COx water at 50 °C).

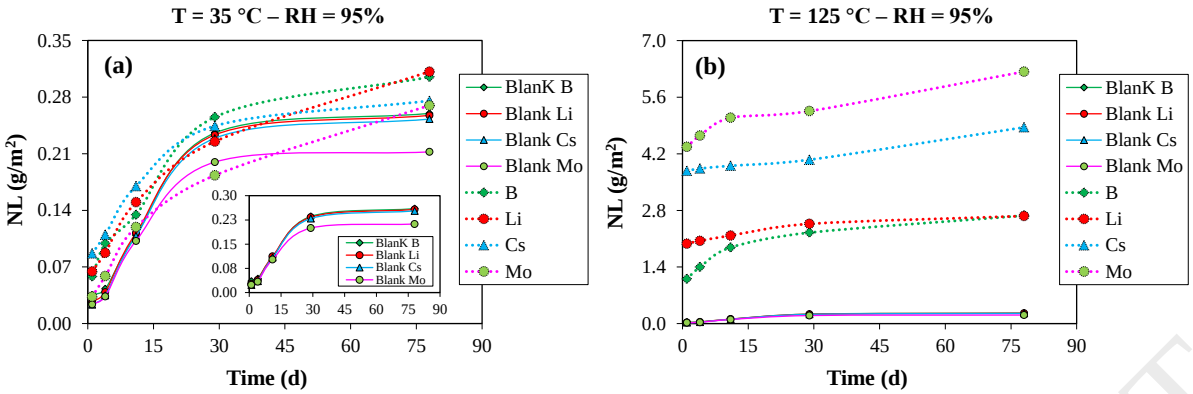

Fig. 13. Evolution with time of the normalized mass loss of glass elements (*NL*, g m^{-2}) for samples hydrated for 766 days under 95% RH and at 35 (a) and 125 °C (b), and then leached in COx water at 50 °C for 78 days.

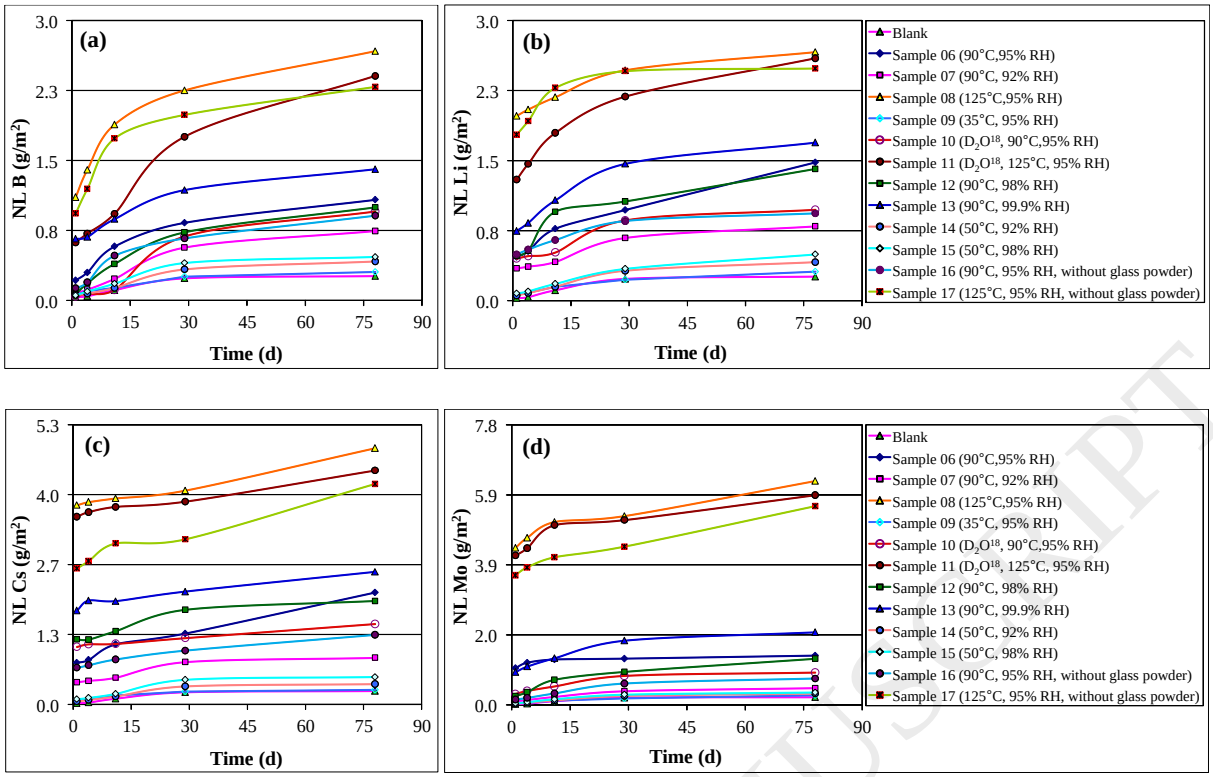

Fig. 14. Evolution with time of the normalized mass loss of B (a), Li (b), Cs (c) and Mo (d) for all SON68 glass samples hydrated under various conditions and then leached in COx water for 78 days at 50 °C.

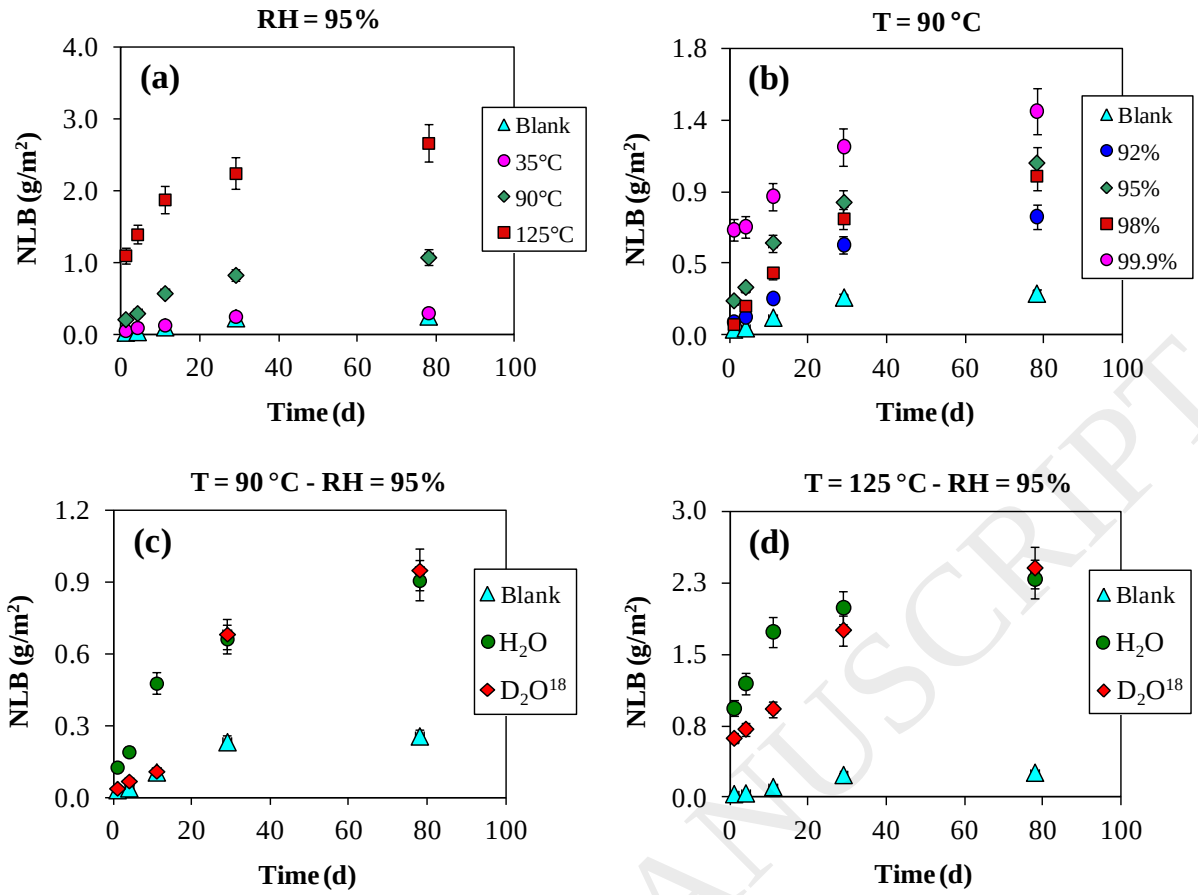

Fig. 15. Evolution of the normalized mass loss of boron (*NLB*, g m^{-2}) as a function of time for leaching experiments in COx water of pre-hydrated SON68 glass monoliths at: different temperatures and 95% RH (a); different relative humidities and 90 °C (b); 95% RH and 90 °C (c) and 125 °C (d) in H_2O and D_2O^{18} (20%).

Table 1
Chemical composition in weight% of the inactive simulated French nuclear waste glass SON68.

Oxide	Wt %	Oxide	Wt %	Oxide	Wt %
SiO_2	45.85	ZnO	2.53	Nd_2O_3	2.04
B_2O_3	14.14	P_2O_5	0.29	Pr_2O_3	0.46
Na_2O	10.22	SrO	0.35	Ag_2O	0.03
Al_2O_3	5.00	ZrO_2	2.75	CdO	0.03
CaO	4.07	MoO_3	1.78	SnO_2	0.02
Li_2O	1.99	Cs_2O	1.12	TeO_2	0.23
Fe_2O_3	3.03	BaO	0.62	Ce_2O_3	0.97
NiO	0.43	Y_2O_3	0.20	Others	0.39
Cr_2O_3	0.53	La_2O_3	0.93		

Table 2
Composition of water in equilibrium with the claystone at 50 °C [21]

Component	Concentration (mmol/L)
Cl	41
S(VI)	14
Na	42
K	1
Ca	9.9
Mg	4.1
Sr	0.2
Si	0.35
TIC	3.05

Table 3
Comparison between the alteration gel layer thicknesses for all samples, obtained by the different methods (FTIR, SEM and SIMS). SIMS experiments were performed only for experiments #11 and #17.

Experiment number	**Hydration Conditions**	Alteration time (d)	Gel layer thickness (µm)		
			FTIR	SEM	SIMS
06	T (90 °C) RH (95%)	832	2.12 ± 0.2	1.9 ± 0.2	-
07	T (90 °C) RH (92%)	766	1.66 ± 0.15	1.4 ± 0.2	-
08	T (125 °C) RH (95%)	766	2.57 ± 0.25	4.2 ± 0.4	-
09	T (35 °C) RH (95%)	766	0.31 ± 0.03	0.4 ± 0.1	-
10 (without glass powder)	D_2O^{18} (90 °C) RH (95%)	766	2.05 ± 0.21	1.7 ± 0.2	-
11 (without glass powder)	D_2O^{18} (125 °C) RH (95%)	593	4.9 ± 0.48	4 ± 0.4	3.8
12	T (90 °C) RH (98%)	653	2.42 ± 0.22	2.4 ± 0.3	-
13	T (90 °C) RH (99.9%)	653	2.55 ± 0.25	2.5 ± 0.3	-
14	T (50 °C) RH (92%)	490	0.41 ± 0.04	0.5 ± 0.1	-
15	T (50 °C) RH (98%)	490	0.61 ± 0.06	0.7 ± 0.1	-
16 (without glass powder)	T (90 °C) RH (95%)	490	1.59 ± 0.15	1.5 ± 0.2	-
17 (without glass powder)	T (125 °C) RH (95%)	322	2.67 ± 0.26	2.5 ± 0.3	2.4

Table 4
The average initial and long-term rates of the glass hydration measured by FTIR method for different temperatures and relative humidity values.

		Sample 09: 35 °C (95% RH)	**Sample 14: 50 °C (92% RH)**	**Sample 06: 90 °C (95% RH)**	**Sample 08: 125 °C (95% RH)**
Initial hydration rate (before plateau)	Period	(0–766 days)	(0–490 days)	(0–652 days)	(0–593 days)
	HR_0 (g m^2 d^{-1})	1.1 (± 0.1) × 10^{-3}	2.2 (± 0.2) × 10^{-3}	8.2 (± 0.8) × 10^{-3}	1.1 (± 0.1) × 10^{-2}
Long-term hydration rate (after plateau)	Period	not reached	not reached	(652–832 days)	(593–766 days)
	$HR_{L\text{-}T}$ (g m^2 d^{-1})			1.4 (± 0.1) × 10^{-3}	1.0 (± 0.1) × 10^{-3}

Table 5
Water diffusion coefficient D_{H2O} obtained from the evolution of the alteration layer thickness based on FTIR measurements.

	Sample 06: 90 °C (95% RH)	**Sample 09: 35 °C (95% RH)**	**Sample 14: 50 °C (92% RH)**	**Sample 15: 50 °C (98% RH)**	**Sample 11: D_2O^{18}, 125 °C (95% RH)**	**Sample 17: 125 °C (95% RH) without powder**
Time (d)	574	766	490	490	593	490
r^2 (-)	0.9797	0.8341	0.9575	0.985	0.9847	0.9617
D_{H2O} (m^2 s^{-1})	7.5 (± 0.6) × 10^{-20}	8.7 (± 0.7) × 10^{-22}	3.2 (± 0.3) × 10^{-21}	7.28 (± 0.6) × 10^{-21}	5.3 (± 0.4) × 10^{-19}	3.8 (± 0.3) × 10^{-19}